EFFECT OF CALCINATION DURATION TOWARDS THE PHYSICAL AND CHEMICAL PROPERTIES OF MOLYBDENUM-DOPED VANADIUM PHOSPHORUS OXIDE CATALYST

OW CHUN ONN, JONATHAN

A project report submitted in partial fulfilment of the requirements for the award of the degree of Bachelor of Engineering (Hons.) Chemical Engineering

Faculty of Engineering and Science
Universiti Tunku Abdul Rahman

June 2010

DECLARATION

I hereby declare that this project report is based on my original work except for citations and quotations which have been duly acknowledged. I also declare that it has not been previously and concurrently submitted for any other degree or award at UTAR or other institutions.

Signature : _____

Name : Ow Chun Onn, Jonathan

ID No. : 07 UEB 05050

Date : _____

APPROVAL FOR SUBMISSION

I certify that this project report entitled **"EFFECT OF CALCINATION DURATION TOWARDS THE PHYSICAL AND CHEMICAL PROPERTIES OF MOLYBDENUM-DOPED VANADIUM PHOSPHORUS OXIDE CATALYST"** was prepared by **OW CHUN ONN, JONATHAN** has met the required standard for submission in partial fulfilment of the requirements for the award of Bachelor of Engineering (Hons.) Chemical Engineering at Universiti Tunku Abdul Rahman.

Approved by,

Signature : _____

Supervisor : Dr. Leong Loong Kong

Date : _____

Specially dedicated to
my beloved mother and father,
my friends, and supervisor.

ACKNOWLEDGEMENTS

I would like to thank everyone who had contributed to the successful completion of this project. I would like to express my gratitude to my research supervisor, Dr. Leong Loong Kong for his invaluable advices, guidance and his enormous patience throughout the development of this research.

In addition, I would also like to express my gratitude to God who has given me peace and wisdom, my loving parent who are always supportive and gave me guidance, and my friends who had helped and given me encouragement in completing this project. Through this project, I've learnt that it is difficult to rely on my own strength and knowledge, but with the help from my supervisor and friends, my burden has been made easy.

Again, I would like to sincerely thank everyone who had contributed directly or indirectly to the completion of this project.

EFFECT OF CALCINATION DURATION TOWARDS THE PHYSICAL AND CHEMICAL PROPERTIES OF MOLYBDENUM-DOPED VANADIUM PHOSPHORUS OXIDE CATALYST

ABSTRACT

This project is aimed at investigating the effect of different calcination duration on molybdenum dopant towards the physical and chemical properties of vanadium phosphorus oxide (VPO) catalyst. A series of 0.1 % Mo-doped vanadyl pyrophosphate catalysts with calcination duration of 24 h, 48 h, 72 h, and 96 h were prepared via sesquihydrate route, which exhibited a well crystallized $(VO)_2P_2O_7$. These catalysts are denoted as VPO24, VPO48, VPO72, and VPO96. Increasing the calcinations duration in *n*-butane/air mixture led to an increasing trend in surface area which is 13.4 $m^2 g^{-1}$ (VPO24), 16.9 $m^2 g^{-1}$ (VPO48), 17.6 $m^2 g^{-1}$ (VPO72), and 22.1 $m^2 g^{-1}$ (VPO96). SEM showed a trend whereby the longer the calcinations duration is, catalysts with increasing amount rosette-type of agglomerate characteristics were produced. Redox test showed an increasing V_{avg} from 4.2750 (VPO24) to 4.2804 (VPO48) and to 4.3700 (VPO72) but decreases to 4.2483 (VPO96). This showed that the formation of V^{5+} increased from 24h to 72h, but decreased at 96h.

TABLE OF CONTENTS

LIST OF TABLES

LIST OF FIGURES

LIST OF SYMBOLS / ABBREVIATIONS

c_p	specific heat capacity, J/(kg·K)
h	height, m
K_d	discharge coefficient
M	mass flow rate, kg/s
P	pressure, kPa
P_b	back pressure, kPa
R	mass flow rate ratio
T	temperature, K
v	specific volume, m^3
α	homogeneous void fraction
η	pressure ratio
ρ	density, kg/m^3
ω	compressible flow parameter
ID	inner diameter, m
MAP	maximum allowable pressure, kPa
MAWP	maximum allowable working pressure, kPa
OD	outer diameter, m
RV	relief valve

LIST OF APPENDICES

CHAPTER 1

INTRODUCTION

1.1 Catalysis and Catalysts

Catalysis (pronounced cat-AL-uh-sis) is the process by which some substance is added to a reaction in order to make the reaction occur more quickly. The substance that is added to produce this result is the catalyst (pronounced CAT-uh-list).

A catalyst is a chemical substance that affects the rate of a chemical reaction by altering the activation energy required for the reaction to proceed. This is called catalysis. A catalyst is not consumed by the reaction and it may participate in multiple reactions at a time. The only difference between a catalyzed reaction and an uncatalyzed reaction is that the activation energy is different. There is no effect on the energy of the reactants or the products [Helmenstine, 2001].

For example, catalytic converter is a device used in car exhausts systems to remove gases which cause air pollution. The catalytic converter obtained its name from the fact that certain metals (the catalysts) inside the device causes the exhaust gases to break down. For instance, when potentially dangerous nitrogen (II) oxide passes through a catalytic converter, platinum and rhodium catalysts will cause the oxide to break down into harmless nitrogen and oxygen. Under normal circumstances, nitrogen (II) oxide will break down into nitrogen and oxygen even without the presence of platinum and rhodium but this process takes place over hours, days, or weeks and as time passes, the dangerous gas is already in the atmosphere. In

the catalytic converter, the breakdown of nitrogen (II) oxide takes place within a matter of seconds [Science Clarified, 2010].

1.2 Types of Catalysis

1.2.1 Homogeneous Catalysis

Catalysis reactions are usually categorized as either homogeneous or heterogeneous reactions. A homogeneous catalysis reaction is one in which both the catalyst and the substances on which it works are all in the same phase (solid, liquid, or gas).

The reaction of ozone break-down by chlorine atoms is an example of homogeneous catalysis.

$$Cl + O_3 \rightarrow ClO_3$$
$$ClO_3 \rightarrow ClO + O_2$$
$$ClO + O \rightarrow Cl + O_2$$

Ozone can decompose spontaneously under the influence of light, but a chlorine atom accelerates the reaction. The chlorine atom reacts at the same gas phase as the ozone and at the end of the reaction, chlorine atom leaves the reaction unaltered. Hence, the chlorine atom is known as a homogeneous catalyst [Chorkendorff *et al.*, 2003].

1.2.2 Heterogeneous Catalysis

A heterogeneous catalysis reaction is one in which the catalyst is in a different phase from the substances on which it acts. Heterogeneous catalysis is the more common type of the two types of catalysis.

In a catalytic converter, for example, the catalyst is a solid, usually a precious metal such as platinum or rhodium. The substances, on which the catalyst acts, however, are gases, such as nitrogen (II) oxide and other gaseous products of combustion. Another industrial example would be the production of benzene from the dehydrogenation of cyclohexane using platinum-on-alumina as the catalyst [Science Clarified, 2010].

1.3 Energy Profile of Reaction with Catalysts

In order for two species to react together, they have to come in contact and collide against each other before they may react. The collisions between the species have to be in the correct orientation and overcome a certain minimum energy called the activation energy which is the minimum energy required before a reaction can occur. For an over-all exothermic reaction, the ***energy profile*** looks like this:

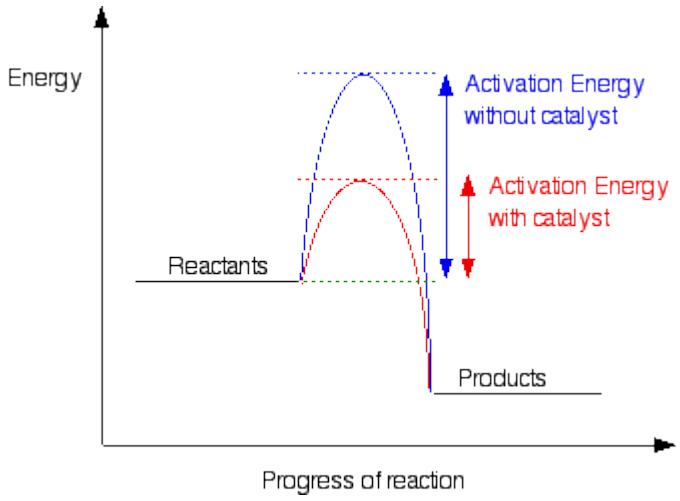

Figure 1.1: Energy versus Progress of reaction with catalyst

The only difference between an exothermic reaction and an endothermic reaction are the product and reactant lines. For an endothermic reaction, the products have higher energy than the reactants causing the green arrow to be pointing upwards.

The rate of a reaction can be increased by increasing the number of successful collisions. One possible way of doing this is to provide an alternative way for the reaction to happen which has a lower activation energy. Adding a catalyst has this exact effect on activation energy. A catalyst provides an alternative route for the reaction and this alternative route has lower activation energy as shown in Figure 1.1 [Clark, 2002].

In any system, particles present have a very wide range of energies. Therefore, it would be useful to know the proportion of the particles present which have enough energy to react. For gases, the Maxwell-Boltzmann Distribution graph shows the distribution particle energies in each particle.

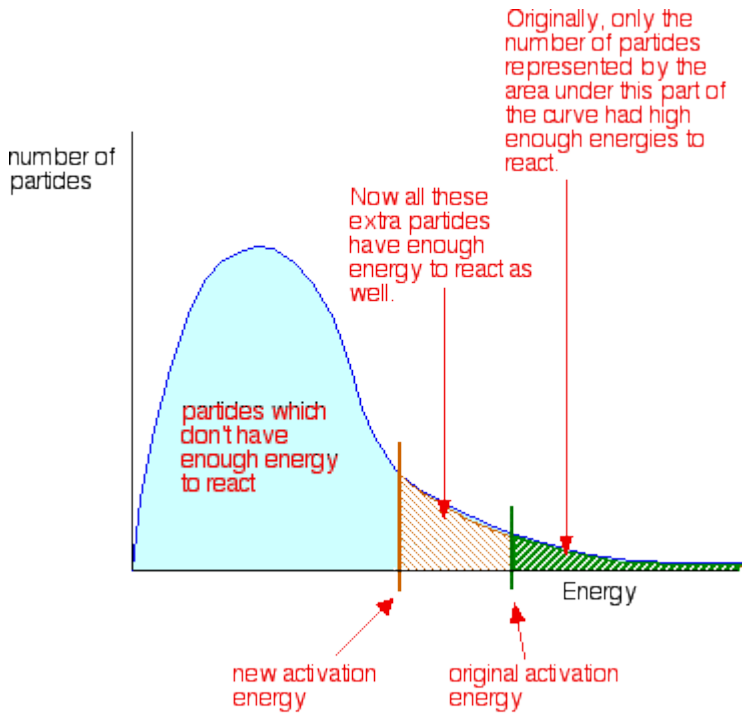

Figure 1.2: Maxwell-Boltzmann Distribution Graph

From the Maxwell-Boltzmann Distribution graph, it is noticed that only a handful of particles have energy which is high enough to react. In order for more particles to react, the activation energy has to be shifted to the left or to change the shape of the curve. By adding a catalyst which gives an alternative route with lower activation energy, more particles are able to react and the Maxwell-Boltzmann Distribution graph becomes shifted to the left [Clark, 2002].

1.4 Essential Properties of Good Catalysts

There are several properties that a good catalyst should have:

1. Large surface areas
2. Variable coordination number - This defines the number of nearest neighbours an atom or molecule can bind to. Having a variable number allows potential catalyst to link extra molecules at the surface when reactants are adsorbed and to release them again when the reaction is complete
3. Variable oxidation state - This is the number of electrons an element can donate or receive. By taking part in electron exchange a potential catalyst can initiate chemical changes in molecules that bind to its surface. The electron exchange can also promote the binding of the molecules to its surface in the first place
4. Ability to vary its stereochemistry - This defines the angles between bonds and this can affect the shapes of molecules that can be created
5. Remains stable under reaction condition
6. Affinity strong enough for the incoming monomer but not too strong that it is difficult to persuade them to react or detach from the catalyst surface
7. Long active life – This defines how long it can be used before it becomes deactivated by poisons, or loses its mechanical stability
8. High selectivity - The extent to which it produces the desired product rather than any other by products
9. High activity – The speed at which it makes the reaction go

[Source: IMPRESS Education, 2009]

1.5 Importance and Uses of Catalysts

Many important chemical reactions require inputs of energy to proceed. If a catalyst is present, less energy will be required to complete the reaction.

A catalyst is important in many industrial processes. One of the most common commercial catalyst processes is the Haber process where ammonia, a primary component of many fertilizers, is produced economically with the use of iron oxide which speeds up the reaction. The conversion of nitrogen and hydrogen into ammonia is practically impossible above 600 °C but higher temperature is needed to break the very strong triple bond in nitrogen gas. Other than that, the reaction between hydrogen and nitrogen is so slow that it is economically unviable without a catalyst. By adding iron as catalyst in the process, the conversion speeds up and the breaking of triple bond in nitrogen gas are possible at lower temperature. Another example where catalyst plays an important role in industries is the production of sulfuric acid, which is used to produce batteries, detergents, dyes, explosives, plastics, and many other produces, is commonly produced using a catalyst called vanadium oxide [Schlogl, 2008].

Other than being an important element in industries, catalysts also play a crucial part in preserving and protecting the environment. Automobiles use catalytic converters to treat exhaust where metals such as platinum and palladium facilitate the chemical conversion of noxious gases to more inert forms, greatly decreasing the environmental impact of combustion engines [Epson, 1993].

Probably the most important impact of catalyst is on life itself. All important biochemical reactions are catalyzed by molecules called enzymes. Most enzymes are proteins which catalyze specific reactions within cells. Some examples include polymerases, which synthesize Deoxyribonucleic Acid (DNA) and Ribonucleic Acid (RNA), peptidases, which digest protein, and ATP syntheses, which produce energy for the many different cell activities [Epson, 1993].

1.6 Problem Statements

The problem of this study is to obtain the optimum calcination duration for vanadium phosphorus oxide (VPO) catalyst doped with molybdenum dopant. Vanadium phosphorus oxide (VPO) is the only system capable of oxidizing *n*-butane to maleic anhydride which is the single largest manufacture of unsaturated polyester resins used in fibre-reinforce plastics, and manufacturing of alkyd resins used in paints and coatings with good selectivity. To increase the activity of the catalyst, promoters are added to improve the mechanical resistance and catalytic properties.

This problem requires further research in order to obtain solution in the industrial level. This qualitative study will explore the surface and morphology of the molybdenum-doped VPO catalyst to find out the optimum condition in producing good VPO catalyst. By using various analysis equipments, the presence of different phases, surface morphology and other properties of the catalyst which affects the activity and selectivity of the catalyst can be determined.

1.7 Objectives of Research

- To synthesise Molybdenum-doped VPO catalyst
- To examine the physical and chemical properties of VPO doped with molybdenum dopant
- To determine the optimum calcination duration for the Mo-doped VPO catalyst

CHAPTER 2

LITERATURE REVIEW

2.1 Vanadyl Pyrophosphate Catalyst $(VO)_2P_2O_7$

Vanadium Phosphorus Oxide (VPO) has been used for the selective oxidation of lower alkanes such as *n*-butanes since the mid 1970's, and the nature of the active catalyst has been the object of extensive research [Centi *et al*., 1988]. Many crystalline phases exist in the VPO system and correlations of catalytic activity with crystalline structure have been reviewed by many authors such as Birkeland *et al*., and Volta *et al*. Vanadyl pyrophosphate has been identified as the main crystalline phase present in the most selective and active VPO catalyst for *n*-butane oxidation to maleic anhydride [Bordes and Courtine, 1979].

Vanadyl pyrophosphate is prepared from a precursor, vanadyl (IV) hydrogen phosphate hemihydrates, $VOHPO_4 \cdot 0.5H_2O$ in an *n*-butane/air gas mixture at about 400^oC for an extended time period. Calcination in nitrogen causes loss of water and the transformation of the hemihydrates into the pyrophosphate. The precursor can be prepared from either aqueous or alcoholic solution. The choice of preparation medium alters the morphology of the hemihydrates and in turn the composition and the morphology of the final VPO catalyst, ultimately determining the catalyst performance [Horowitz *et al*., 1988].

The preparation of vanadyl pyrophosphate from vanadyl (IV) hydrogen phosphate hemihydrates, $VOHPO_4 \cdot 0.5H_2O$ in an *n*-butane/air gas mixture consists of a complex mixture of phases such as α-, β-, γ-$VOPO_4$, $VOHPO_4 \cdot 4H_2O$, $VOHPO_4\ 0.5H_2O$, $VO(PO_3)_2$ and β-, γ- $(VO)_2P_2O_7$ [Birkeland *et al.*, 1997]. The combinations of some V^{5+} phases ($VOPO_4$) and a V^{4+} phase [$(VO)_2P_2O_7$] are a necessary requirement if the catalyst is to simultaneously indicate good activity and selectivity [Hutchings *et al.*, 1998 and Coulston *et al.*, 1997]. Wang *et al*. (2001) have confirmed these observations and further demonstrated that selective oxidation of *n*-butane over VPO catalysts takes place via a Mars–van Krevelen mechanism in which the VPO catalyst surface cations cycle under steady state reaction conditions between V^{4+} and V^{5+}.

The presence of different crystalline phases observed in the VPO catalyst is due to several parameters which are:

1. temperature, time, and atmosphere of activation
2. morphology of the precursor
3. P/V ratio in the precursor
4. presence of defects in the structure

Vadim and Moises (2005) concluded that the most active and selective phase for n-butane oxidation was related to the crystalline $(VO)_2P_2O_7$ characterised by the preferential exposure of the surface (2 0 0) planes and a slight excess of phosphate (P/V = 1.01-1.10). The active and selective surface sites for *n*-butane oxidation to maleic anhydride were associated with the presence of vanadyl dimers in the surface (2 0 0) planes of $(VO)_2P_2O_7$.

Volta *et al.* (1987) believed that the active sites are not associated with interfaces between these crystalline phases. They suggested that the active phase for selective oxidation of *n*-butane consists of a mixture of well-crystallized $(VO)_2P_2O_7$ and an amorphous $V^{5+}OPO_4$ phase involving corner-sharing VO_6 octahedral (Figure 2.1A). This amorphous phase was interpreted as a precursor of b-$VOPO_4$, which was formed at higher reaction temperatures.

Hutchings *et al*. (1998) and Volta *et al*. (1997) suggested that the actives sites for *n*-butane oxidation to maleic anhydride comprise a V^{4+}/V^{5+} couple well dispersed on the surface of a range of VPO phases. Hutchings *et al.* (1998) also included the possibility that the actives sites could be the defects found by Gai and Kourtakis (1995) as well as interfaces between microcrystalline $VOPO_4$ phases and well-crystalline $(VO)_2P_2O_7$.

Yamazoe *et al*. (1990) reported $VO(H_2PO_4)_2$ as the precursor of the active and selective phase in *n*-butane oxidation. This precursor transformed to an amorphous $VO(PO_3)_2$ catalyst which is much less active but just as selective as the $(VO)_2P_2O_7$ catalysts (Figure 2.1B).

Trifiro *et al.* (1988) attributed the activity of the VPO catalysts in *n*-butane oxidation to vanadyl pyrophosphate, whereas the selectivity to maleic anhydride was associated with the presence of a very limited and controlled amount of V^{5+} sites (Figure 2.1C). Trifiro *et al*. (1988) suggested that the active surface is obtained by truncation of the $(VO)_2P_2O_7$ crystals along the (2 0 0) plane.

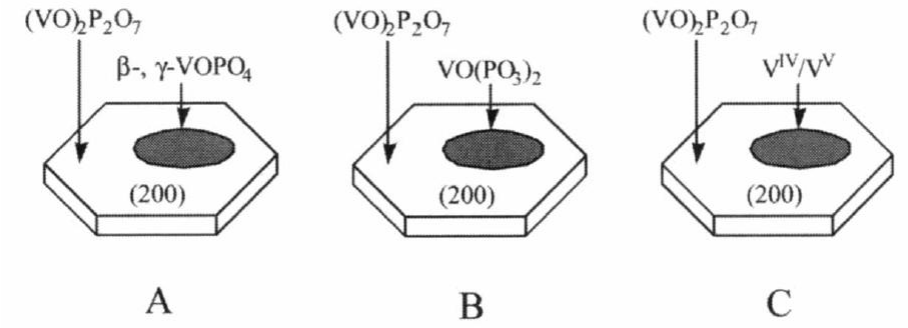

Figure 2.1: Vanadium Pyrophosphate and the phases present in (2 0 0) planes as suggested by A) Volta *et al.* (1997) B) Yamazoe *et al*. (1990) C) Trifiro *et al*. (1988)

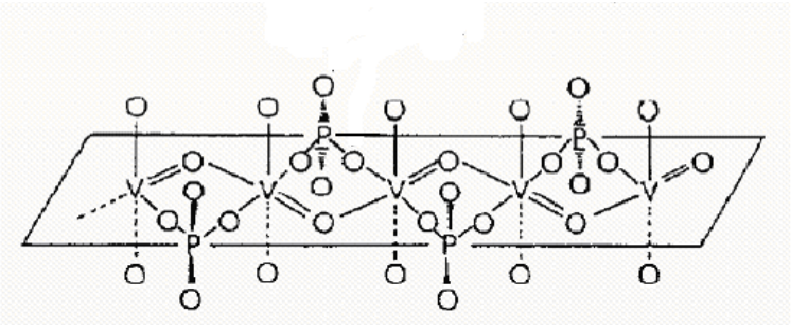

Figure 2.2: Ideal orientation of Vanadium Pyrophosphate phase

2.2 Preparation of Vanadium Phosphorus Oxide Catalyst

There are several methods to prepare Vanadium Phosphorus Oxide and different methods influence the behaviour and the characteristics of the catalyst. In all the methods used to prepare the catalyst, the difference could be due to a few parameters which are: Vanadium/phosphorus (P/V) ratio; Activation procedure; and conditioning procedure.

According to Centi *et al*., 1988, in order to obtain an optimal catalyst, the necessary conditions are:

1. Synthesis of microcrystalline $(VO)HPO_4.0.5H_2O$ prepared in organic solvent and this is characterised by a preferential exposure of the basal plane (0 0 1).
2. The presence of defects in stacking of the platelets.
3. Slight excess of phosphorus with respect to the stoichiometric amount with an atomic P/V ratio in the range of 1.01 to 1.10.

There are many methods to prepare the VPO catalyst such as by thermal dehydration of vanadyl (IV) hydrogen phosphate hemihydrates, aerosol processing where aerosol created by air of an aqueous solution of NH_4VO_3 and H_3PO_4 at 700 °C, and many other methods. The most common method is by using V_2O_5 as a source of vanadium, and H_3PO_4 is used as a source of phosphorus. Different reducing agents which result in different kinds of precursors can be used and the precursors will transform to vanadyl pyrophosphate catalyst after the calcination process at high temperature. Different methods of preparation will produce catalyst with different specific surface area, whereas the nature of active sites was not affected by the preparation methods [Shima and Hatano, 1997]. VPO catalysts can also be prepared via aqueous medium, organic medium, dihydrate precursor route, hemihydrate precursor route, and sesquihydrate precursor route.

2.2.1 Aqueous Medium

In aqueous medium, a reducing agent is required to synthesis the V^{4+} precursor phase. V_2O_5 is reduced by a mineral agent such as HCl or N_2H_4 in water and phosphoric acid is added. As a result, the precursors prepared are more crystalline. After calcination, the precursors produced a low specific surface area (10 m^2g^{-1}) catalyst [Harrison *et al.*, 1976]. In an aqueous medium, the formation of the precursor proceeds through a sequence of steps. During the reaction, vanadium pentoxide is suspended with 85% aqueous *otho*-phosphoric acid, *o*-H_3PO_4 in distilled waterto obtain the desired P/V atomic ratio and vanadyl phosphate dihydrate, $VOPO_4 \cdot 2H_2O$ is obtained as an intermediate before obtaining the precursor. The solid (precursor) was dried at 150 ℃ overnight, and then calcined. [Taufiq Yap *et al*., 2001].

When vanadium phosphorous oxide (VPO) catalyst is prepared via aqueous medium, the final catalyst tends to have low surface area where the catalyst activity is directly proportional to surface area. Therefore, these catalysts exhibit poor performance for butane oxidation [Hutchings, 2004].

2.2.2 Hemihydrate Precursor Route

Felthouse *et al*. (2001) proposed that the most effective catalyst, Vanadium Phosphorus Oxide, is produced during the pyrolysis of vanadyl (IV) hydrogen phosphate hemihydrate (VHP). Vanadyl (IV) hydrogen phosphate hemihydrate is obtained by thermal dehydration from vanadyl pyrophosphate.

Hemihydrate precursor ($VOHPO_4\ 0.5H_2O$) can be prepared via aqueous medium or organic medium. Both methods use the same reactants, but different reducing agent. In an aqueous method, the hemihydrate precursor is prepared by reducing V_2O_5 solid with an aqueous solution of HCl in the presence of H_3PO_4. While in an organic method, the hemihydrate precursor forms by the reaction of

V_2O_5 with H_3PO_4 in benzyl alcohol/isobutanol. Both reactions will end by a water extraction step [Cavani *et al*., 1994].

2.2.3 Dihydrate Precursor Route

Dihydrate precursor, $VOPO_4{\cdot}2H_2O$, method was first proposed by Horowitz *et al*. (1988) and further described by Johnson *et al*. (1984). Hutchings *et al*. (1997) have reported that very active catalysts can be prepared using a two-stage method based on $VOPO_4{\cdot}2H_2O$, which is known as the VPD route. According to Bartley *et al.* (2001), dihydrate precursor ($VOPO_4{\cdot}2H_2O$), as a starting point for catalyst preparation, is ready to achieve effective control of the hemihydrate precursor ($VOHPO_4{\cdot}0.5H_2O$) morphology. Synthesis of dihydrate is of crucial importance with respect to the subsequent precursor preparation and catalytic performance.

This method is based on the reaction of V_2O_5 with H_3PO_4 and water act as solvent which leads to the formation of the V^{5+} dehydrate phase $VOPO_4{\cdot}2H_2O$ [Hutchings, 2004]. The dihydrate is recovered and dried, then refluxed in a second step with alcohol to form the hemihydrate. The alcohol used in the second step to reduce $VOPO_4{\cdot}2H_2O$ to $VOHPO_4{\cdot}0.5H_2O$ can produce catalyst precursors with better morphology and texture. Therefore, VPD route can give the $(VO)_2P_2O_7$ phase with the highest surface platelet morphology exposing preferentially the (1 0 0) active plane for maleic anhydride formation [Hutchings *et al.*, 1997].

By using dihydrate precursor as a starting material for the preparation of VPO catalysts, the precursor will leads to the synthesis of two types of materials. One of them is by providing a method which produces a high surface area form of $VOHPO_4{\cdot}0.5H_2O$ that can topotactically transform to a high surface area final catalyst comprising mainly of $(VO)_2P_2O_7$. Besides, the precursor also provides a new route to the synthesis of $VO(H_2PO_4)_2$ which in turn has been found to provide ultra-selective catalysts for the synthesis of maleic anhydride [Hutchings *et al.*, 1997].

2.2.4 Organic Medium

In organic medium, vanadium with H_3PO_4 is emulsified in alcohol such as benzyl alcohol and isobutyl alcohol. The vanadium oxide-alcohol mixture is refluxed for 3 hours at 120℃ under continuous stirring. The mixture is then cooled to room temperature and left stirring overnight. 99% *o*-H_3PO_4 is added in a quantity such as to obtain the expected P/V atomic ratio. The resulting solution is again heated to 120℃ and maintained under reflux with constant stirring for 2 hours. Then the slurry (precursor) is filtered, washed, dried at 150 ℃, and the final product is in the form of fine powder. Particles are characterized by dimensions of smaller crystallites [Centi *et al.,* 1983].

Catalysts prepared in an organic medium will show a higher specific reactivity as they present not only a higher surface area but also a greater density of active sites [Cavani and Trifiro, 1994]. By using organic medium in the preparation of this catalyst, there are possibilities of obtaining high values of surface area of precursors which can be increased by calcinations at 380^{o}C, and characterized by a lower oxidability in air at high temperature. The morphology of organic precursors depends on the nature of the solvent/reducing agent (an aliphatic or benzylic alcohol), the synthesis P/V ratio, the time and temperature of reduction, and the amount of water present during synthesis.

2.2.5 Sesquihydrate Precursor Route

Recently, a new alternative route in preparing vanadyl pyrophosphate catalyst has been developed through vanadyl hydrogen phosphate sesquihydrate precursor ($VOHPO_4 \cdot 1.5H_2O$). The sesquihydrate precursor was obtained by reducing $VOPO_4 \cdot 2H_2O$ in 1-butanol. After calcinations, it had shown high specific activity in selective oxidation of n-butane to maleic anhydride [Taufiq-Yap *et al*., 2004]. Employing 1-butanol as solvent, the sesquihydrate could be intercalated with dopants to afford modified $(VO)_2P_2O_7$ with high activity and selectivity to maleic anhydride.

The synthesis of sesquihydrate precursor has been divided into a two-step procedure involving $VOPO_4 \cdot 2H_2O$ as an intermediate before obtaining the precursor. In the first step, vanadyl phosphate dihydrate, $VOPO_4 \cdot 2H_2O$ is prepared by reacting V_2O_5 with aqueous *o*-H_3PO_4 in distilled water. The mixture is then stirred under reflux. The resultant solid is then recovered by using the centrifuge technique and subsequently washed sparingly with distilled water and oven dried.

In the second step, $VOPO_4 \cdot 2H_2O$ is added to 1-butanol and refluxed. After cooled to room temperature, the resultant precipitates is centrifuged out from the solvent, washed sparingly with acetone, and dried in an oven to obtain the sesquihydrate precursor [Taufiq-Yap *et al*., 2004].

2.3 Parameters of Vanadium Phosphorus Oxide Catalyst

There are several parameters which affect the performance of the VPO catalyst which are: calcination condition; support system; dopant; and P/V atomic ratio. These parameters are essential as they change the surface area and morphology of the catalyst which in turn affects the activity and selectivity.

2.3.1 Parameter: Calcination Conditions

Calcination and activation are critical steps in the transformation of vanadyl hydrogen phosphate hemihydrate (VPO precursor – $VOHPO_4\ 0.5H_2O$) to vanadyl pyrophosphate (VPO catalyst – $(VO)_2P_2O_7$). Calcination conditions can be varied in temperature, pressure, duration, and gas-phase composition which affect the surface area, oxidation state, and catalytic activity.

Perez *et al*. (1996) have suggested that when the calcination temperature is increased, the crystallinity of VPO also increases. The crystal size in the VPO increased with the calcination temperature, but phosphorus content causes a diminution in the particle size. On the other hand, the phosphorus content increased the specific area of the VPO. Catalyst performance declines with increasing pressure, but the pressure−time relationship allows a range of conditions: Optimal catalytic performance was achieved within 20 h of calcination at atmospheric pressure, but it took less than 4 h to achieve this high level of performance when precursor was calcined at 3.5 atm (at longer times, the catalytic performance deteriorated). Co-feeding steam (in the presence of oxygen) generally had a deleterious effect on catalyst performance and, in particular, maleic anhydride yield. Moreover, oxidation states higher than 4.5 were achieved with steam/oxygen mixtures in as little as 20 h. Catalyst performance declined linearly with oxidation state for precursor which are calcined to vanadium oxidation states exceeding 4.5 [Patience *et al.*, 2007].

2.3.2 Parameter: Support System

Support system in VPO catalyst is a method to increase the yield and selectivity of the catalyst towards the conversion of *n*-butane to maleic anhydride. In the case of supported catalysts, the active phase is spread over rough, powdered support materials to obtain thermostability, a maximum surface area and coarse bodies that are suitable for use in reactors. The way in which an active phase is spread over the support material determines its accessibility and its practical value in terms of reactivity. Therefore, many studies have been devoted to the determination of the dispersion, wetting and interaction of active species with support materials [van Santen *et al*., 1999].

The advantages of using a support system on the catalyst are: (i) strong thermal stability suitable for the highly exothermic reaction, (ii) large pore diameter to minimize pore diffusion resistance, and (iii) the positive support-catalyst interaction to make the supported VPO more selective to maleic anhydride production [Kuo and Yang, 2004]. Mahdavi *et al*. (2010) also pointed out that potentially; supported VPO catalysts have advantages over the unsupported ones, including better heat transfer characteristics, larger surface area to volume ratio of active component, better mechanical strength, and controllable catalyst textures. Materials such as SiO_2, TiO_2, Al_2O_3, MCM-41 and Al-MCM-41 have been used in attempts to support VPO.

2.3.3 Parameter: Dopant

Dopants which are also known as promoters, is a popular choice in VPO catalyst to improve the surface area and morphology of the catalyst to increase the reactivity and selectivity. Dopants are widely used in catalyst but the exact role of each element is mostly unknown and controversial [Pierini and Lombardo, 2005].

Mode of addition of the promoters has been investigated by Batis *et al*. (1996) whereby the additions of promoters are based on thermal addition, Lewis-acid-promoted addition and others. Promoter electronegativity on the other hand has been stressed by Takita *et al*. (2000) whereby the activity of the catalyst is based on the charge and electron acceptor property. Next, the generation of defects was investigated by Ye *et al*. (2006); the redox character by Abon *et al*. (1997), and acidity by Zazhigalov *et al*. (1993).

Other aspects includes formation of solid solution as molybdenum phosphate ($MoOPO_4$) and $VOPO_4$ are iso-structural phases thus a small amount of solid formation of Mo and V mixed phase could have been formed during stabilization period, and formation of amorphous phase [Pierini and Lombardo, 2005].

From a mechanical view, strong Lewis acid sites which favours hydride abstraction which is the rate determining step could be a $V^{4+\delta+}$ site stemming from defects in the structure of the vanadyl pyrophosphate [2 0 0] plane according to Centi *et al*. (1993), and Volta *et al*. (1998) also pointed out the this site could be a V^{5+} center either dispersed in the same phase or from a $VOPO_4$ phase.

Never-the-less, most authors researched and concluded that the addition of dopants into the VPO catalysts increased the surface area of the catalysts and induced the formation of V^{5+} phases which are shown in XRD and LRS spectra that promoted the catalytic performance [Pierini and Lombardo, 2005].

2.3.4 Parameter: P/V Atomic Ratio

During the preparation of VPO catalyst, it has been found that the P/V atomic ratio plays an important role in the reaction over VPO catalysts [Ballarini *et al*., 2006]. However, there is a lack of discussion about the structure of these catalysts and details of the conversion in different condition.

Tousi and Mahdavi (2010) found that the organic medium synthesis is a favorable method for production of the catalyst and both of the activity and selectivity are directly dependent to the P/V ratio in the structure of the catalyst. This effect is related to the increasing of the surface area and crystallity of VPO sample and enhancement of the acidity of Bronsted (P–OH) and Lewis acid sites (V^{4+}). In the presence of Lewis acid sites (V^{4+}) the H-abstraction occurs and the cleavage of C–H bond occurs on Bronsted acid sites (P–OH). Bronsted acidity favors the stabilization of intermediates and the generation of an organic surface species that is involved in oxygen activation.

2.4 Maleic Anhydride

Maleic anhydride is the anhydride of *cis*-butenedioic acid (maleic acid) where the carboxylic acid groups are next to each other in the *cis* form. Maleic Anhydride has a cyclic structure with a ring containing four carbon atoms and one oxygen atom. It is soluble in acetone and hydrolyzes in water. It is an organic compound with the formula $C_2H_2(CO)_2O$ and in its pure state, it is a colourless or white solid with an acrid odour. Maleic anhydride was traditionally produced by oxidation of benzene and due to the rise in benzene prices and its poisonous nature, *n*-butane is used as a replacement [Cavani and Teles, 2009].

Maleic anhydride has an attractive molecule structure in chemistry. Its reactivity of the two carbonyl groups and the solid bond in conjugation with the two carbonyl oxygens provide broad commercial applications. Examples of reactions which maleic anhydride are involved in:

- Acylation
- Alkylation
- Amidation
- Cycloaddition
- Decomposition and Decarboxylation
- Diels-Alder reaction
- Electrophilic Addition and Nucleophilic Addition
- Ene Reaction
- Esterification
- Formation of Acid Chloride
- Grignard Reactions
- Halogenation
- Heterogeneous catalytic reduction
- Hydration and Dehydration
- Hydroformylation
- Isomerization
- Ligation
- Michael Addition
- Ozonolysis and Oxidaton
- Polymerization

[Source: ChemiCalland, 2009]

2.4.1 Uses of Maleic Anhydride

Maleic anhydride (MA) is widely used in polyester resin production as MA is an important intermediate for the processing unsaturated polyester. Polyesters are used in many fiber-reinforced plastics; materials with a wide and growing range of application in boating, automobile, and construction industries. It is also used as a co-monomer for unsaturated polyester resins, an ingredient in bonding agents used to manufacture plywood, a corrosion inhibitor, and a preservative in oils and fats.

Other than polyesters, MA is also important in producing alkyl resins which are used in paints and coatings. MA is also important in producing succinic anhydride, maleic acid, 1, 4-butanediol, THF, and butirolactone. Moreover, it is used as an additive of lubricant oils, which are used in gasoline and diesel engine crankcase oils as dispersants and corrosion inhibitors [PrimaryInfo.com, 2009].

A smaller application of MA would be in food industry. The food industry uses MA in artificial sweeteners and flavour enhancements. Personal care products consuming MA includes hair sprays, adhesives and floor polishes. MA is also used in water treatment chemicals, detergents, certain agricultural chemicals such as insecticides and fungicides, pharmaceuticals and copolymers. [ChemiCalland, 2009]

2.4.2 Oxidation of *n*-butane to Maleic Anhydride

Recent processes for manufacturing maleic anhydride employ C_4 hydrocarbons, such as *n*-butane and *n*-butylene, as feedstocks. Even existing processes which originally use benzene as a reactant are converting to using C_4 hydrocarbons. A major advantage of C_4 hydrocarbons over benzene is that no carbon is lost in the reaction to form MA. For a theoretically achievable conversion of 100%, the yield from butane is a third greater than that from benzene. From the raw material viewpoint, the relatively low purchase price of C_4 is much more attractive than the expensive benzene [Lee, 2009].

Other influential factors which favour C_4 are safety, health, and the environment. Benzene is a known carcinogen and one of the most stringently regulated chemical by the government. The flammability limits for C_4 hydrocarbons are also lower than those of benzene, which is an additional safety advantage of the process. For all of these reasons, the fixed-bed process with *n*-butane has been the only MA route used commercially since 1985 in the United States [Lee, 2009].

2.4.2.1 Reaction Details

The commercially predominant butane oxidation process employs a fixed-bed, but processes using fluidized beds and transport beds are also being developed. In the fixed-bed process, a low concentration of butane is passed over the catalyst in tubular reactors similar to the benzene process. The selective reaction is given below:

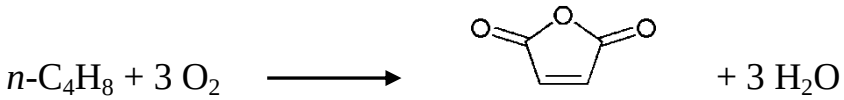

The reactor is operated at temperatures between 400 – 480 °C, and the pressure is held at 0.3 - 0.4 MPa to force the exit gases downstream for scrubbing and purification. Unlike the benzene process, only a small amount of the MA can be condensed from the reactor effluent due to the increased formation of water. The remaining product is washed out as maleic acid in a scrubber and then dehydrated to reform MA. An alternative recovery method absorbs the MA from the reaction gas by organic solvents. The MA is then distilled from the high boiling solvent in a fractional distillation column [Lee, 2009].

CHAPTER 3

METHODOLOGY AND CHARACTERISATION TECHNIQUES

3.1 Materials and Gases used

Below are the chemicals used throughout this study:

1. Vanadium (V) pentoxide, V_2O_5 (UNI Chem)
2. *Ortho*-Phosphoric acid, *o*-H_3PO_4 (85%) (MERCK)
3. 1-Butanol, $CH_3(CH_2)_3OH$ (R&M Chemicals)
4. Molybdenum Oxide, MoO_3 (Systerm)
5. Nitric Acid, HNO_3 (R&M Chemicals)
6. Sulphuric Acid, H_2SO_4 (95-98%) (Systerm)
7. Potassium permanganate, $KMnO_4$ (Hmbg Chemicals)
8. Ammonium iron (II) sulphate, $(NH_4)_2Fe(SO_4)_2$ (R&M Chemicals)

The gases used throughout this study:

1. 0.75% *n*-butane in air (Malaysia Oxygen Berhad (MOX))
2. 99.99% Purified Nitrogen (Malaysia Oxygen Berhad (MOX))
3. 99.99% Purified Helium (Malaysia Oxygen Berhad (MOX))
4. 99.99% Purified Argon (Malaysia Oxygen Berhad (MOX))
5. Liquid Nitrogen (Malaysia Oxygen Berhad (MOX))

3.2 Methodology

Generally, the preparation of the bulk vanadyl pyrophosphate catalysts can take place via different routes; notably the sesquihydrate precursor route (VPOs), the organic route (VPOo) and the reduction on Vanadyl phosphate dehydrate, $VOPO_4 \cdot 2H_2O$ phase (VPOd). The preparation of the doped vanadyl pyrophosphate catalysts can take place via organic route and the reduction of $VOPO_4 \cdot 2H_2O$ phase. In this research, the preparation of the vanadium phosphorus oxide catalyst takes place via the sesquihydrate precursor $VOHPO_4 \cdot 1.5H_2O$.

3.2.1 Preparation of the Vanadyl Phosphate Dihydrate ($VOPO_4 \cdot 2H_2O$)

The producing of vanadyl pyrophosphate catalyst has been developed via vanadyl hydrogen phosphate sesquihydrate precursor, $VOHPO_4 \cdot 1.5H_2O$ [Matsuura *et al.*, 1995]. The synthesis of sesquihydrate precursor has been divided into two-step procedure, which involving vanadyl phosphate dehydrate, $VOPO_4 \cdot 2H_2O$ as an intermediate before obtaining the precursor.

Firstly, 15 g of vanadium pentoxide, (V_2O_5) was weighed. It was then added with 90 ml of *ortho*-phosphoric acid, *o*-H_3PO_4 (85%) and 360 ml of distilled water. The mixture was then refluxed for 24 hours at 120 °C. A yellow intermediate will be formed. The mixture was cooled to room temperature and was centrifuged. Yellow solids recovered by centrifuge technique, were washed sparingly with acetone and were oven dried (~80 °C) for 24 hours. The yellow solids obtained are vanadyl phosphate dehydrate ($VOPO_4 \cdot 2H_2O$).

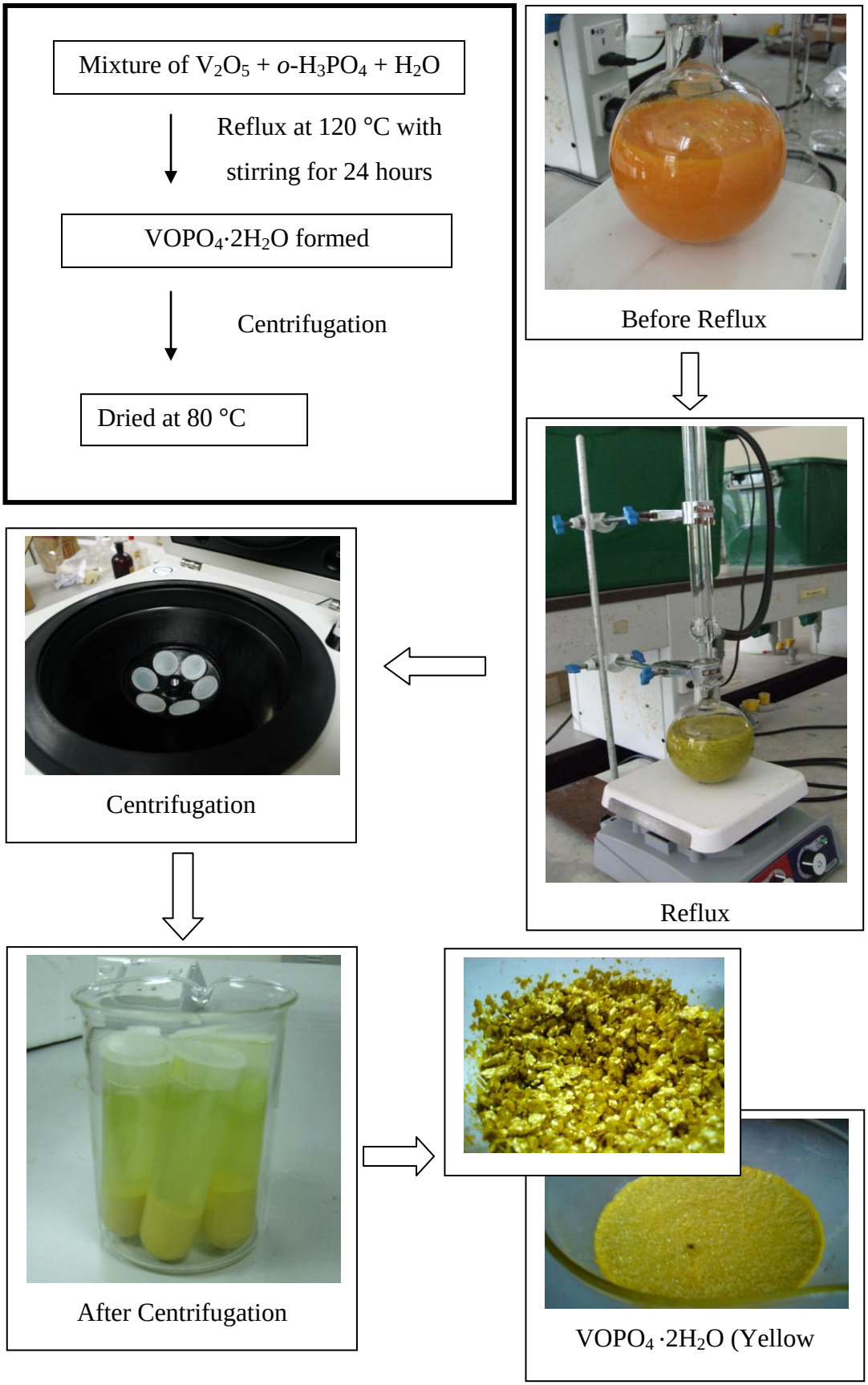

Figure 3.1: Diagram shows the preparation steps of $VOPO_4 \cdot 2H_2O$ (Yellow Solid)

3.2.2 Preparation of the Mo-doped Vanadium Phosphorus Oxide Catalysts

10 g of $VOPO_4 \cdot 2H_2O$ precursors were added with 150 ml 1-butanol and 0.00646 g of Molybdenum Oxide, (MoO_3). The mixture was then under reflux for 24 hour. After being cooled to room temperature, the resultant precipitate which is whitish-blue powder is referred to vanadyl hydrogen phosphate sesquihydrate precursor with 0.1% Molybdenum. Whitish-blue powder was recovered by centrifuge technique, washed sparingly with acetone and oven dried at 80 °C for 24 hours.

The resulting powder was then undergone calcination in a reaction flow of 0.75% *n*-butane in air mixture at 400 °C respectively for each of the following durations; 24 hours, 48 hours, 72 hours, and 96 hours.

The calcined molybdenum doped (Mo-doped) catalysts were denoted as 0.1%MoVPOs-24h, 0.1%MoVPOs-48h, 0.1%MoVPOs-72h, and 0.1%MoVPOs-96h, where 0.1%Mo = 0.1% of molybdenum relative to vanadium, VPOs = sesquihydrate precursor route of preparation, and 24h = calcinations duration. All the Mo-doped catalysts was calcined at the same temperature (460 °C), therefore it is not stated in the denotation. For simplicity, 0.1%MoVPOs-24h is referred as VPO24, 0.1%MoVPOs-48h is referred as VPO48, 0.1%MoVPOs-72h is referred as VPO72, and 0.1%MoVPOs-96h is referred as VPO96.

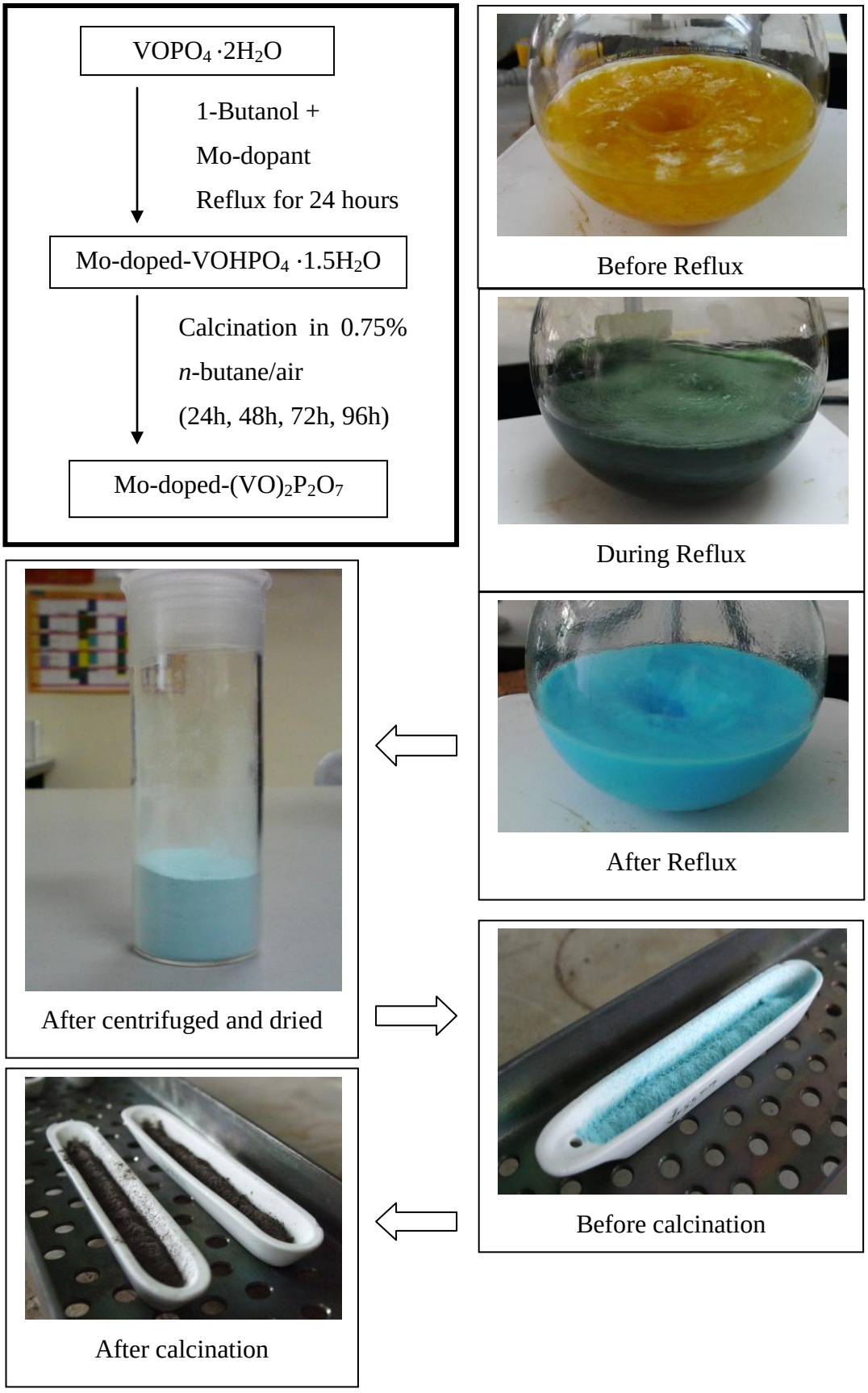

Figure 3.2: Diagram shows the preparation steps of Mo-doped Vanadium Phosphorus Oxide Catalyst

3.3 Characterisation Techniques and Instrumentations

Throughout the research, there are some instruments involved to examine the physical and chemical properties of the catalysts produced. They are used to analyse the catalyst formed, which is the vanadyl pyrophosphate catalyst. The machines and techniques used are notably, X-Ray Diffractometer (XRD), BET surface area measurements, Scanning Electron Microscopy (SEM), and Redox Titration.

3.3.1 X-Ray Diffraction (XRD) Analysis

X-Ray Diffraction (XRD) Analysis is a machine used to determine the phase composition of catalysts at ambient temperature and under normal atmospheric conditions. It is one of the most powerful and efficient techniques for qualitative and quantitative analysis of crystalline compounds. It relies on the dual wave or particle nature of X-Rays to obtain information about the structure of crystalline materials. The sample is prepared for analysis by packing a small amount of sample into a shallow cup. Sometimes the samples can be introduced as slurry and placed on a quartz slide [DeltaLab, 1998].

The phenomenon of diffraction occurs when the penetrating radiation, X-Rays enters a crystalline substance and is scattered. The scattered X-Rays will undergo constructive and destructive interference in a process termed as diffraction. In order for a beam to be 100% diffracted, the distance it travels between rows of atoms at the angle of incident must be equal to an integral multiple of the wavelength of the incident beam. D-spacings which are greater or lesser than the wavelength of the directed X-Ray beam at the abgle of incidence will produce a diffracted beam of less than 100% intensity. Sample will rotate during the analysis to reduce any heating to the sample. Resulting diffractogram will confirm the identity of a solid material as a pharmaceutical powder. The diffraction of X-Ray by crystals is described by Bragg's Law. X-Rays are reflected from a crystal only if the angle of incidence satisfies the condition $n\lambda = 2d \sin \theta$ [Harris, 2007].

X-Ray diffraction has been in use in two main areas: the fingerprint characterization of crystalline materials and the determination of their structure. Each crystalline solid has its unique characteristic X-Ray powder pattern which may be used as a "fingerprint" for its identification. Once the material has been identified, X-Ray crystallography may be used to determine its structure, *i.e.* how the atoms pack together in the crystalline state and what the interatomic distance and angles are. Therefore, size and shape of the unit cell for any compound most easily determined by using the diffraction of X-Rays. In catalysis, X-Ray diffraction analysis is carried out to determine the phase compositions of catalysts at ambient temperature and under normal atmospheric conditions. Therefore, the relative abundance of V^{4+} and V^{5+} can be determined. The crystallite sizes can also be determined by using Debye-Scherrer equation:

$$t = \frac{0.89\,\lambda}{\beta_{hkl}\cos\theta_{hkl}}$$

where t is the crystallite size for (*h k l*) phase, λ is the X-Ray wavelength of radiation for CuKα, $\beta_{h\,k\,l}$ is the full-width at half maximum (FWHM) at (*h k l*) phase and $\theta_{h\,k\,l}$ is the diffraction angle for (h k l) phase [Klug and Alexander, 1974].

In this study, X-Ray diffraction (XRD) patterns were obtained using a Shimadzu diffractometer model XRD-6000 (Figure 3.3) employing CuKα radiation generated by a Philips glass diffraction X-Ray tube broad focus 2.7 kW type on the catalysts at ambient temperature. The basal spacing was determined via powder technique. The sample were scanned at the range $2\theta = 2° - 60°$ with a scanning rate of 1.2000 ° min^{-1}. The diffractograms obtained were matched against the Joint Committee on Powder Diffraction Standards (JCPDS) PDF1 database version 2.6 to confirm the catalysts phases.

The analysis starts by performing calibration using a silicon sample as standard. After calibration, catalyst sample is slotted into the X-Ray column for analysis. Calibration and sample analysis takes about 15 minutes and 45 minutes respectively.

Figure 3.3: Shimadzu diffractometer model XRD-6000

3.3.2 BET Single Point Surface Area Measurement

The Brunauer-Emmett-Teller (BET) single point analysis involves the nitrogen adsorption at low temperature has been used for the determination of the single point surface area of porous materials. The Sorptomatic 1990 is based on the static volumetric principle to characterize solid samples by the technique of gas adsorption. It is designed to perform both physisorption and chemisorption enabling determination of the total specific surface area, porosity and the specific surface area.

Adsorption is defined as the concentration of gas molecules near the surface of a solid material. The adsorbed gas is called *adsorbate* and the solid where adsorption takes place is known as the *adsorbent*. Adsorption is a physical phenomenon (usually called physisorption) that occurs at any environmental condition (pressure and temperature) but only at very low temperature it becomes measurable. Thus physisorption experiments are performed at very low temperature, usually at the boiling temperature of liquid nitrogen at atmospheric pressure [CE-Instrument UK, 2001].

Adsorption takes place because of the presence of an intrinsic surface energy. When a material is exposed to a gas, an attractive force acts between the exposed surface of the solid and the gas molecules. The result of these forces is characterized as physical (or Van der Waals) adsorption, in contrast to the stronger chemical attractions associated with chemisorption. The surface area of a solid includes both the external surface and the internal surface of the pores [CE-Instrument UK, 2001].

Due to the weak bonds involved between gas molecules and the surface (less than 15 KJ/mole), adsorption is a reversible phenomenon. Gas physisorption is considered non-selective, thus filling the surface step by step (or layer by layer) depending on the available solid surface and the relative pressure. Filling the first layer enables the measurement of the surface area of the material, because the amount of gas adsorbed when the mono-layer is saturated is proportional to the entire surface area of the sample. The complete adsorption/desorption analysis is called an adsorption isotherm [CE-Instrument UK, 2001].

The six IUPAC standard adsorption isotherms are shown in Figure 3.4. They differ because the systems demonstrate different gas/solid interactions [CE-Instrument UK, 2001].

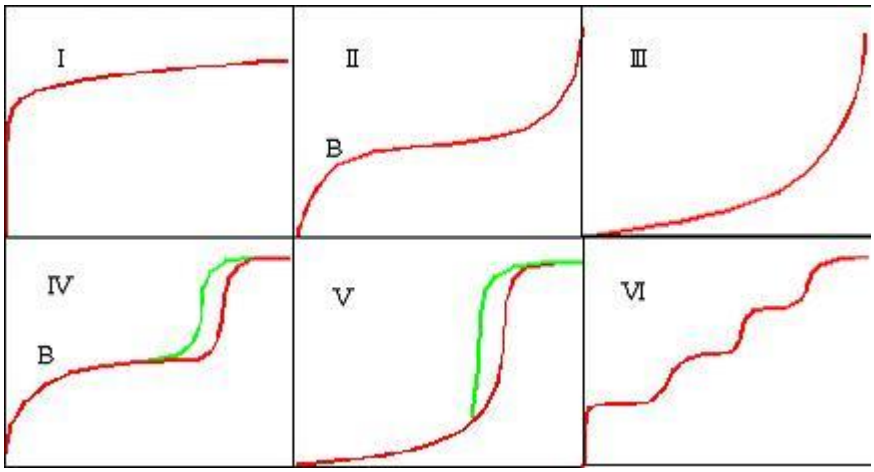

Figure 3.4: Six IUPAC standard adsorption isotherms

The Type I isotherm is typical of microporous solids and chemisorption isotherms. Type II is shown by finely divided non-porous solids. Type III and type V are typical of vapor adsorption (i.e. water vapor on hydrophobic materials). Type VI and V feature a hysteresis loop generated by the capillary condensation of the adsorbate in the mesopores of the solid. Finally, the rare type VI step-like isotherm is shown by nitrogen adsorbed on special carbon [CE-Instrument UK, 2001].

Brunauer, Emmett and Teller introduced an adsorption model that allows for adsorption in multilayer in 1938. The concept of BET theory is actually a variants of Langmuir isotherm (monolayer adsorption) modified to fit multilayer adsorption [Moulijn *et al.*, 1993]. Thus the assumptions made in deriving Langmuir isotherm is applied which are all adsorption sites are equally active, surface of adsorbent is flat, no interaction between each adsorption layer and between the adsorbed molecules itself, gas molecules physically adsorbed on a solid in layers infinitely, and lastly, adsorbed molecules are localized (immobile).

For BET analysis, the empty sample tube is first degassed for at least 30 minutes. Once finished, the vacuumed-empty sample tube is weighted as blank. Then, 0.5 gram of sample is added into the sample tube and degassed overnight. Once done, the sample tube is weighted and the actual sample mass is taken as: (Tube + sample weight) – (blank weight). The sample tube with sample inside is then connected to the analysis port. Liquid nitrogen is filled and the gas used for blank analysis is helium. Follow the steps for operating the Sorptomatic 1990 software to run blank analysis. For sample analysis, the sample tube with sample inside is again degassed overnight and then connected to the analysis port. Liquid nitrogen is filled and the gas used for sample analysis is nitrogen. Follow the steps for operating the Sorptomatic 1990 software to run sample analysis.

Figure 3.5: Sorptomatic Series 1990

3.3.3 Redox Titration

This method was developed by Miki Niwa and Yuichi Murakami in 1982. They had investigated the reaction mechanism of the ammoxidation of toluene on V_2O_5 / Al_2O_3 catalyst. The bi-functional activity of this catalyst which consists of the oxidation activity of V_2O_5 and the dehydration property of Al_2O_3 is stressed. However, some problems about the activity sites of vanadium oxide and alumina and how they actually contribute to the ammoxidation of toluene remain a question [Niwa and Murakami, 1982].

In this research, redox titration was carried out to determine the average vanadium valance (AV) of the VPO catalysts and/or to obtain the average oxidation state of vanadium. First, a known amount of the sample is dissolved in 100 ml sulphuric acid (2 M). It is then cooled to room temperature before being titrated with potassium permanganate solution (0.01 N). This titrant is used to oxidise V^{3+} and V^{4+} in the solution to V^{5+}. The end point is reached when the change of colour from the original greenish blue to pink was observed. The volume of potassium permanganate used was recorded as V_1. Then the oxidised solution was treated with ammonium iron (II) sulphate solution (0.01 N). This is to reduce V^{5+} to V^{4+} in the solution. Diphenylamine is used as an indicator. The end point is reached when the purple colour of the solution disappeared and became colourless. The volume of ammonium iron (II) sulphate used was recorded as V_2 [Niwa and Murakami, 1982].

Another fresh 25 ml of the original solution was then treated with 0.01 N ammonium iron (II) sulphate solution. Diphenylamine is also used as indicator. This stage of titration is to determine the V^{5+} in the original solution. The end point is reached when the solution changes from purple to greenish blue. The volume of ammonium iron (II) sulphate solution used was recorded as V_3.

The average oxidation state of vanadium (AV) can be determined by solving the equation below:

$$AV = \frac{5V^{5+} + 4V^{4+} + 3V^{3+}}{(V^{5+} + V^{4+} + V^{3+})}$$

where V^{3+}, V^{4+}, and V^{5+} are concentration of vanadium at different oxidation state. In order to obtain the values for V^{3+}, V^{4+}, and V^{5+} respectively, the following equations are used:

$$V^{3+} = 20(0.01)V_1 - 20(0.01)V_2 + 20(0.01)V_3$$
$$V^{4+} = 40(0.01)V_2 - 40(0.01)V_3 - 20(0.01)V_1$$
$$V^{5+} = 20(0.01)V_3$$

where V_1 = the volume of potassium permanganate used and V_2 = the volume of ammonium iron (II) sulphate used.

[Niwa and Murakami, 1982]

Figure 3.6: Redox Titration

3.3.4 Inductively Coupled Plasma-Optical Emission Spectrometer (ICP-OES)

The bulk and doped catalyst chemical composition was determined by using a sequential scanning inductively coupled plasma-optical emission spectrometer (ICP-OES) Perkin Elmer Optical Emission Spectrometer Optima 7000 DV. A solution of the sample is fed into a plasma where it is ionised. As well as ionising the sample, it also excites the atoms and ions. Over a short space of time, the atoms lose that excitation energy in the form of light. ICP-OES measures the intensity of light at the various wavelengths characteristic of particular elements to determine their concentration [Robinson, 2009].

Main function of an ICP-OES is to 'excite' the outer shell electrons in atoms to higher energy levels. As they lose excitation energy, they give off light of characteristic wavelengths. The light is focussed and the wavelengths separated by passing it through a prism and diffraction grating. All the wavelengths may be detected and quantitated simultaneously, so many elements can be determined at the same time. Therefore, this is an advantage as many elements emit multiple wavelengths simultaneously and thus we have more choice of wavelengths for each element and can measure multiple elements simultaneously. The disadvantage ICP-OES is that each element emits many wavelengths. Sometimes these wavelengths interfere with those of other elements, making it difficult to quantitate [Robinson, 2009].

The light emitted by the OES follows the Planck-Einstein equation $E = hc/\lambda$, where h is Planck's constant, c is velocity of light and λ is wavelength. Since h and c is a constant, the energy released can be said to be exclusive with the element unique wavelength. Also, the intensity of energy emitted at a chosen wavelength is proportional to the amount (concentration) of that element in the sample being analysed. Thus, by determining the wavelengths emitted and its intensity, we can identify the elements present in the sample using fingerprint matching with a reference standard [Robinson, 2009].

To operate ICP-OES for catalyst samples, V and P calibration curve needs to be done first before calibrating the samples. Molybdenum calibration is also required as the samples are Mo-doped. V solution is first prepared in a 1000 ml by dissolving vanadium pentoxide with distilled water. Then, 125 ml of that mixture is pipette into a 250 ml tube. 10 ml nitric acid is added into the 250 ml tube and distilled water is added until the mixture reaches 250 ml. The procedure repeats itself whereby 125 ml of the new mixture is pipette into a 250 ml tube with 10 ml nitric acid and topped-up till 250 ml with distilled water for another 2 times. A diluted series of 50, 25, 12.5 and 6.25 is obtained for the calibration. The entire procedure is repeated for both P and Mo calibration. Sample preparation also employs the same steps.

The prepared solution is then transferred into smaller test tubes and placed on the test tube stand. Follow the operating steps for the Perkin Elmer Optima 7000 DV software to run the analysis. V and P are calibrated before running the samples.

Figure 3.7: Perkin Elmer Optical Emission Spectrometer Optima 7000 DV

3.3.5 Scanning Electron Microscopy-Energy Dispersive X-Ray Spectroscopy (SEM-EDAX)

In scanning electron microscopy, (SEM) an electron beam is scanned across a sample's surface. When the electrons strike the sample, a variety of signals are generated, and it is the detection of specific signals which produces an image or a sample's elemental composition. The three signals which provide the greatest amount of information in SEM are the secondary electrons, backscattered electrons, and X-rays [Herguth, 2008].

Secondary electrons are emitted from the atoms occupying the top surface and produce a readily interpretable image of the surface. The contrast in the image is determined by the sample morphology. A high resolution image can be obtained because of the small diameter of the primary electron beam [SCIS, 2010].

Backscattered electrons are primary beam electrons which are 'reflected' from atoms in the solid. The contrast in the image produced is determined by the atomic number of the elements in the sample. The image will therefore show the distribution of different chemical phases in the sample. Because these electrons are emitted from a depth in the sample, the resolution in the image is not as good as for secondary electrons [SCIS, 2010].

Interaction of the primary beam with atoms in the sample causes shell transitions which result in the emission of an X-ray. The emitted X-ray has an energy characteristic of the parent element. Detection and measurement of the energy permits elemental analysis (Energy Dispersive X-ray Spectroscopy). EDAX can provide rapid qualitative, or with adequate standards, quantitative analysis of elemental composition with a sampling depth of 1-2 microns. X-rays may also be used to form maps or line profiles, showing the elemental distribution in a sample surface [SCIS, 2010].

Small amount of samples are collected via cotton-bud on the sample holder. Grating is done to the sample holder before inserted into the SEM analysis chamber. Follow the operating steps for Hitachi S3400N software to run and analyse the samples.

Figure 3.8: Hitachi S3400N Scanning Electron Microscopy-Energy Dispersive X-Ray Spectroscopy

CHAPTER 4

RESULTS AND DISCUSSIONS

4.1 X-Ray Diffraction (XRD)

The XRD spectrum of the precursor is shown in Figure 4.1 while Mo-doped catalysts calcined at 460 °C in a reaction flow of *n*-butane in air mixture for 24 h, 48 h, 72 h, and 96h are shown in Figure 4.2 Inspection on the XRD spectrum of the precursor showed the presence of $VOHPO_4 \cdot 1.5H_2O$, which was indicated from the peaks at 2θ = 15.5°, 19.6°, 24.2°, 27.1° and 30.4°. This peaks are in agreement of those reported for the $VOHPO_4 \cdot 1.5H_2O$ phase [Albonetti, 1996 and Hermann, 1997].

Mo-doped catalyst shown in Figure 4.2 are well crystallized $(VO)_2P_2O_7$ phase. The catalysts consist a mixture of $(VO)_2P_2O_7$ and some V^{5+} phases which are the β-$VOPO_4$ observed at 2θ = 21.5° for VPO48, and α_{II}-$VOPO_4$ observed at 2θ = 25.1 ° for VPO72. These peaks belonging to V^{5+} seen in VPO48 and VPO72 is also detected by Y.H. Taufiq-Yap *et al*. at 40 h calcination duration but not at 100 h and 132 h. Longer period of calcination than 72 h decreases the V^{5+} phase, which seems to surface only at 48 h but not at 24 h. Theoretically, increasing the calcinations duration increases the amount of $(VO)_2P_2O_7$. The presence of $(VO)_2P_2O_7$ is characterized by the pyrophosphate lines at 2θ = 23°, 28.45°, and 29.94°. [Taufiq-Yap, 2001]

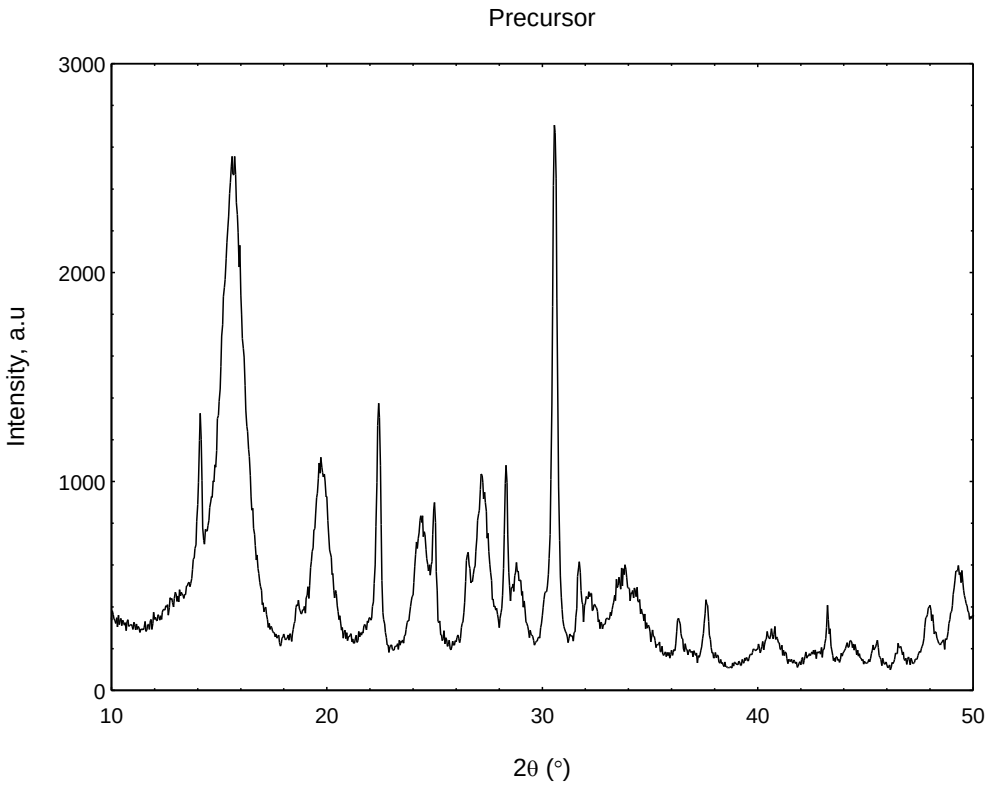

Figure 4.1: XRD patterns of precursor ($VOHPO_4 \cdot 1.5H_2O$)

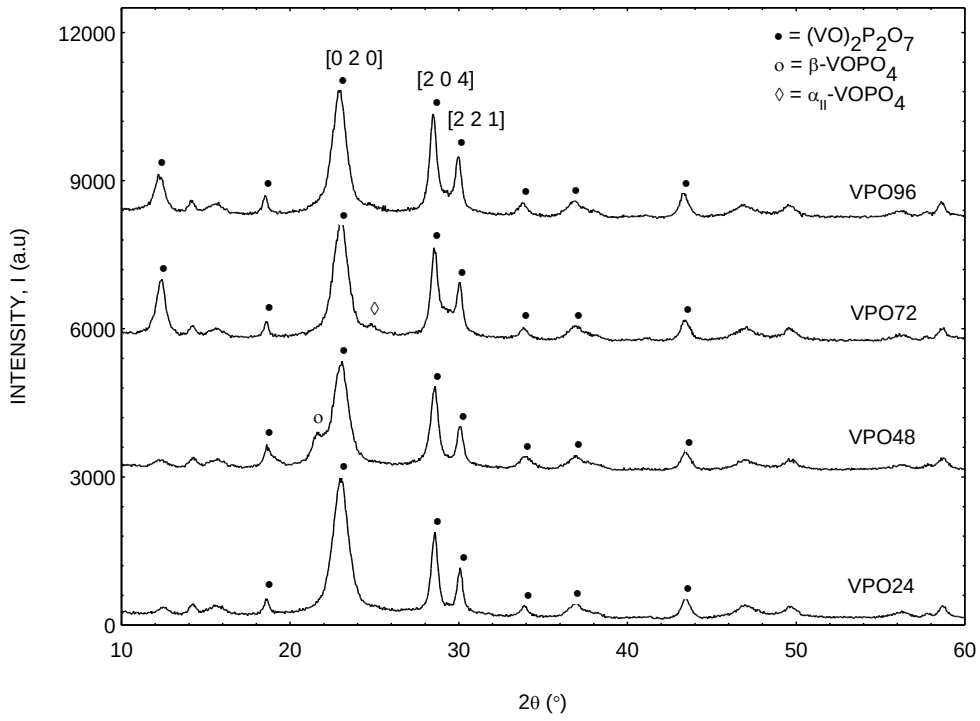

Figure 4.2: XRD patters of Mo-doped VPO catalyst at 24 h, 48 h, 72 h, and 96 h

The FWHM of the (0 2 0) and (2 0 4) planes are used to determine the crystallite size of the catalysts. The line width increases with the decreasing size of the crystallites. The decreasing trend in FWHM of the (0 2 0) planes shows that the thickness of the particles in the (1 0 0) direction decreases. The longer calcination durations produce VPO catalysts with larger crystallite sizes in the (0 2 0) direction but the crystallite sizes in the (2 0 4) direction are almost equal as the difference is small.

Table 4.1: XRD data on Mo-doped VPO catalyst

Catalyst	Line Width[a] (0 2 0) (°)	Line width[b] (2 0 4) (°)	Crystallite Size[c] (0 2 0) (Å)	Crystallite Size[c] (2 0 4) (Å)
VPO24	1.1105	0.6546	72.1683	123.8386
VPO48	1.0926	0.6663	73.3410	121.6006
VPO72	1.0449	0.6438	76.6781	125.8240
VPO96	1.0075	0.6264	79.5459	129.3705

Table 4.1 shows that the crystallite sizes of (0 2 0) planes for VPO24, VPO48, VPO72, and VPO96 are 72.1683 Å, 73.3410 Å, 76.6781 Å, and 79.5459 Å respectively, whereas the crystallite sizes of (2 0 4) planes for the same series are 123.8386 Å, 121.6006 Å, 125.8240 Å, and 129.3705 Å respectively.

4.2 BET Surface Area Measurements and chemical analyses

The surface areas of the Mo-doped catalysts are as follows: 13.4 m^2 g^{-1} for VPO24, 16.9 m^2 g^{-1} for VPO48, 17.6 m^2 g^{-1} for VPO72, and 22.1 m^2 g^{-1} for VPO96 (Table 4.2). Increasing the calcinations duration increases the surface area which is analogous to those reported by Abon *et al*. (1997) and Y.H. Taufiq-Yap *et al*. (2001) for bulk samples.

Chemical analyses confirmed the presence of Mo in catalyst with Mo/V ratios which are 0.004, 0.003, 0.003, and 0.004 for VPO24, VPO48, VPO72, and VPO96 respectively. EDAX results showed that the P/V ratio were in between 0.96 and 1.11 which means the except for VPO72, all other samples have higher phosphorus content than vanadium. ICP-OES indicate that all Mo-doped VPO catalysts have higher phosphorus content than vanadium with P/V ratio in between 1.09 and 1.27. The values are very close as the same amount of Mo dopant is added. The oxidation numbers of vanadium and percentage of V^{4+} and V^{5+} are also shown in Table 4.2. Increasing the calcination durations increased the amount of V^{5+} from 27.5, 28.0 and 37.0 before decreasing to 24.8 while average oxidation number of vanadium increased from 4.275, 4.280 and 4.370 before decreasing to 4.248 for the same series of Mo-doped catalyst. The increment in the average oxidation state of the vanadium from VPO24 to VPO72 is due to the presence of V^{5+} phases before decreasing at VPO96 as shown by the XRD profiles.

Table 4.2: Specific BET surface areas, chemical compositions, average oxidation numbers, and percentages of V^{4+} and V^{5+} oxidation states present in Mo=doped VPO catalyst

Catalyst	Specific BET surface area (m^2 g^{-1})	EDAX	ICP-OES		V^{4+} (%)	V^{5+} (%)	V_{avg}
			P/V	Mo/V			
VPO24	13.4	1.11	1.27	0.004	72.5	27.5	4.275
VPO48	16.9	1.08	1.14	0.003	72.0	28.0	4.280
VPO72	17.6	0.96	1.16	0.003	63.0	37.0	4.370
VPO96	22.1	1.03	1.09	0.004	75.2	24.8	4.248

4.3 Scanning Electron Microscopy (SEM)

The surface morphologies of the Mo-doped catalysts retrieved from the scanning electron microscopy with different calcinations duration are shown in figure 4.3. The principle structures of the catalysts are the rosette-shape agglomerates. Comparing the Mo-doped catalysts samples, there seems to be an increase amount of these rosette-shape agglomerates with increasing calcinations duration. The increase of the surface area for catalysts could be explained by the increase number of platelets which formed the rosette-shape clusters. These plate-like crystallites are comprised of $(VO)_2P_2O_7$ platelets that are exposing the (1 0 0) crystal planes [C.J.Kiely *et al*., 1995].

The size of these rosette-shape agglomerates seems to be decreasing with increasing calcinations duration which explains the contribution to the increase in surface area of the Mo-doped catalyst as found in the BET surface area measurements.

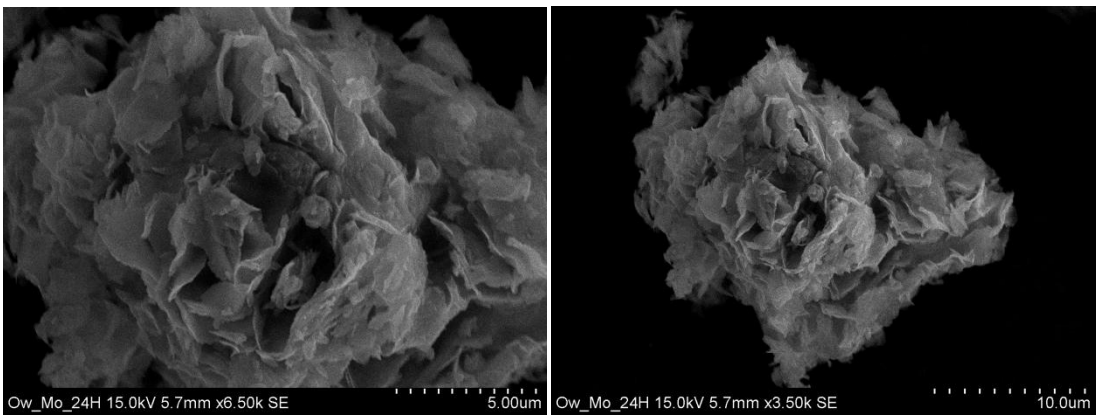

Figure 4.3: SEM micrographs of VPO24 catalyst

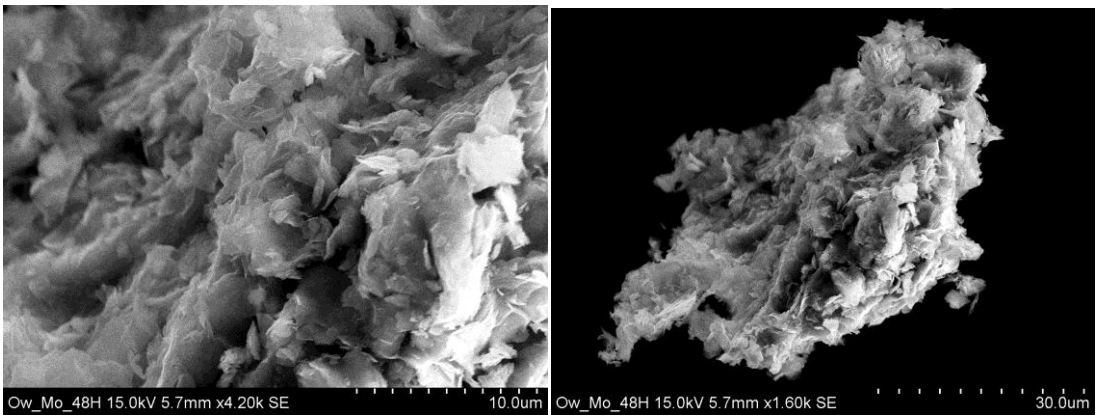

Figure 4.4: SEM micrographs of VPO48 catalyst

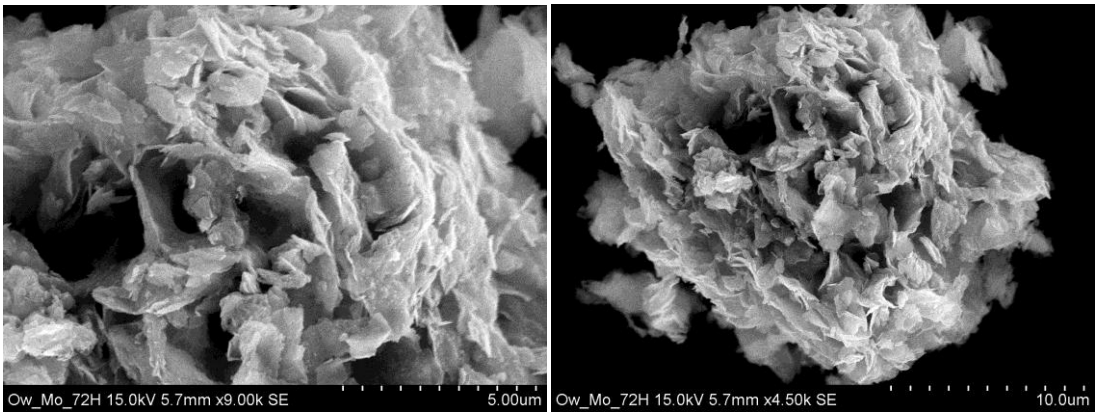

Figure 4.5: SEM micrographs of VPO72 catalyst

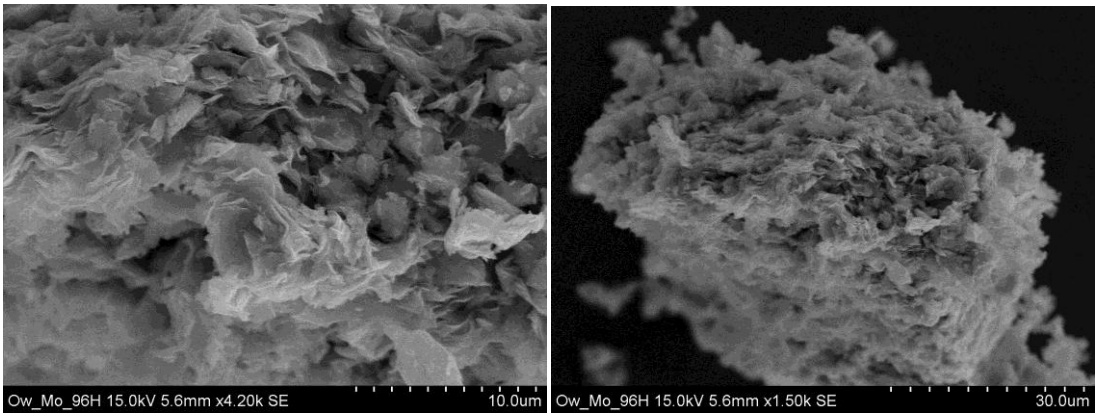

Figure 4.6: SEM micrographs of VPO96 catalyst

CHAPTER 5

CONCLUSIONS AND RECOMMENDATIONS

5.1 Conclusions

Increasing the calcinations duration of vanadyl pyrophosphate catalysts to *n*-butane/air mixture (0.75% *n*-butane) at 460 °C increases the surface area of the catalyst and changes the structure in terms of its bulk morphologies and surface.

Increasing the calcinations duration of Mo-doped catalysts also increases the amount of V^{5+} from VPO24 to VPO72, which increases the catalysts selectivity before it decreases in VPO96.

All the catalysts exhibited good crystalline with characteristic peaks of vanadyl pyrophosphate phase and their surface morphologies were found to be in rosette-shape agglomerates.

EDAX and ICP-OES shows the presence of the compositions in the Mo-doped catalyst series while redox titration and XRD illustrate an increasing trend of V^{5+} amount from VPO24 to VPO72 before it decrease at VPO96 although BET and SEM shows increasing trend of surface area and rosette-shape agglomerates from VPO24 to VPO96.

5.2 Recommendations

This series is not complete without the test using the catalytic reactor. Therefore, it would present a better data and information if the catalytic reactor test is conducted as to support other claims and findings from the entire test conducted. This test could provide information on the reactivity of the VPO catalysts and determine the best catalyst in the series in terms of reaction.

Temperature-programmed desorption, reduction and oxidization (TPDRO) test should also be conducted in order to make concrete the claims of surface area and bulk morphologies from BET and SEM. Although BET test is almost the same as TPDRO, TPDRO provides other information such as the amount of hydrogen reduced and oxygen desorped, which leads to the coverage on the surface of the catalyst, and reduction of activation energy.

REFERENCES

A. Avazpour, V. Mahdavi, L. Avazpour, *Phys. Rev. E* (2010) 82, 041701.

A. Lee, *Manufacturing of Maleic anhydride*, (2009) Louisiana State University. Retrieved from http://www.che.lsu.edu/COURSES/4205/2000/Lee/paper.htm on 11/9/2010.

Anne Marie Helmenstine. *Introduction to Catalysts and Energy Diagrams* (2001). Retrieved from http://chemistry.about.com/od/chemicalreactions/a/catalysts-catalysis.htm on 11/9/2010.

Beatriz T. Pierini, Eduardo A. Lombardo, *Catal. Today* (2005) 107-108, 323-329.

C.J. Kiely, S. Sajip, I.J. Ellison, M.T. Sananes, G.J. Hutchings and J. Volta, *Catal. Lett.* (1995) 33, 357.

CE-Instrument UK, *Sorptomatic 1990 Specifications* (2001). Retrieved from http://saf.chem.ox.ac.uk/Instruments/BET/sorpoptprin.html on 10/12/2010.

ChemiCalland.com, *Maleic anhydride, General Description* (2009). Retrieved from http://chemicalland21.com/petrochemical/MALEIC%20ANHYDRIDE.htm on 11/9/2010.

E. Bordes and P. Courtine, *J. Catal*., (1979) 57-236.

F. Cavani and J.H. Teles, *Chem. SusChem* (2009) 2, 6, 508-534.

F. Cavani, F. Trifiro, *Catalysis*, (1994) 11, 246.

F. Cavani, G. Centi, F. Trifiro, *Ind. Eng. Chem. Prod. Res. Dev*. (1983) 22-570.

G. Bergeret, M. David, J.P. Broyer, J.C. Volta, G. Hecquet, *Catal. Today* (1987) 1, 37.

G. Centi, F. Trifiro, J.R. Ebner, V.M. Francetti, *Chem. Rev*. (1988), 88, 55.

G. Centi, *Vanadyl pyrophosphate catalysts. Catal. Today* (1993) 16, 1 – 5.

G.J. Hutchings, C. Kelly, M.T. Sananes-Schulz, A. Burrows, J.C. Volta, *Catal. Today* (1998) 40, 273-286.

G.J. Hutchings, *Catalyst: Golden Opportunities TCE* (2004) 34-36.

G.W. Coulston, S.R. Bare, H.H. Kung, K. Birkeland, G. Bethke, R. Harlow, P.L. Lee, *Science*, (1997) 275, 191.

H. Morishige, J. Tamaki, N. Miura, N. Yamazoe, *Chem Lett*. (1990) 1513.

H.S. Horowitz, C.M. Blackstone, A.W. Sleight, G. Teufer, *Appl. Catal*, (1988), 38, 193.

I. Matsuura, P. Ruiz, P. Delmon, *Preparation of precursor: New developments in selective oxidation by heterogeneous catalysis* (1995). Amsterdam, Elsevier Science Publisher.

IMPRESS Education. *Catalysts or making it happen* (2011). Retrieved from http://www.spaceflight.esa.int/impress/text/education/Catalysis/index.html on 11/9/2010.

J.K. Bartley, I.J. Ellison, A. Delimitis, C.J. Kiely, A.Z. Isfahani, *Colin Phys. Chem. Chem. Phys*., (2001) 3, 4606-4613.

J.M. Hermann, P. Vernoux, K. Bere and M. Abon, *J. Catal*. (1997) 167, 106.

J.P. Harrison, Jan. P. Hessler, D.R. Taylor, *Phys. Rev. B* (1976) 14, 2979-2982.

J.W. Johnson, D.C. Johnston, A.J. Jacobson, J.F. Brody, *J. Am. Chem. Soc*. (1984) 106: 8123-8128.

Jim Clark. *The Effect of Catalyst on Reaction Rates* (2002). Retrieved from http://www.chemguide.co.uk/physical/basicrates/catalyst.html on 11/9/2010.

K.E. Birkeland, S. Babitz, G. Bethke, H.H. Kung, G.W. Coulston, S.R.Bare, *J. Phys. Chem. B*, (1997) 101, 6895-6902.

L.P. Hammett, *Physical Organic Chemistry* (1970). McGraw Hill, NewYork: Chapter 9.

Lb Chorkendorff, J.W. Niemantsverdriet. Concepts of Modern Catalysis and Kinetics (2003). Wiley-VCH Copyright.

M. Abon and J.C. Volta, *Vanadium phosphorus oxides for n-butane oxidation to maleic anhydride. App. Catal*. (1997). 157, 173 – 193.

M. Niwa and Y. Murakami, *J. Catal*. (1982) 76, 9.

M.T. Sananes-Schulz, A. Tuel, G.J. Hutchings, J.C. Volta, *J. Catal*. (1997) 166, 2, 388.

Michael Epson. *Why is Catalysis Important?* (1993). Retrieved from http://www.pa.msu.edu/sci_theater/ask_st/060993.html on 11/9/2010.

N. Harrouch Batis, H. Batis, A. Ghorbel, *App. Catal*. (1996) 147, 2, 347-361.

P. Gai, K. Kourtakis, *Science* (1995) 267, 5198, 661.

P. Robinson, *A Commercial Analytical Laboratory*, (2009) R. J. Hill Laboratories Ltd., Hamilton. Retrieved from http://nzic.org.nz/ChemProcesses/analysis/15C.pdf on 10/12/2010.

Robert Schlogl. *Handbook of Heterogeneous Catalysis* (2008). Wiley-VCH Verlag GmbH & Co.

S. Albonetti, F. Cavani, F. Trifirò, P. Venturoli, G. Calestani, M.L. Granados and J.L.G. Fierro, *J. Catal*. (1996) 160, 52.

Science Clarified. *Catalyst and catalysis* (2011). Retrieved from http://www.scienceclarified.com/Ca-Ch/Catalyst-and-Catalysis.html on 11/9/2010.

ScienceStuff (2002). *The production of maleic anhydride*. Retrieved from http://www.vanadium.com.au/ScienceStuff/Chemistry/MaleicAnhydride.htm on 3/10/2010.

T.R. Felthouse, J.C. Burnett, B. Horrell, M.J. Mummey, Y.J. Kuo, *Kirk Online* (2001).

V.A. Zazhigalov, J. Haber, J. Stoch, A. Pyanitzkaya, G.A. Komashko, and V.M., *Properties of cobalt promoted $(VO)_2P_2O_7$ in the oxidation of butane. App. Catal.* (1993) 96, 135 – 150.

V.G. Vadim and A.C. Moises. *Catalysis Chapter 1* (2005). RSC Publishing.

W.W Robert and L. S Glenn, *Vanadium-phosphorus-oxygen industrial catalysts for n-butane oxidation: Characterization and kinetic measurements.* (1986) Ind, 25, 612-620

X. Wang, H.Y. Chen, W.M.H. Sachtler, *J. Catal*. (2001) 197, 281.

Y.H. Taufiq-Yap, L.K. Leong, M.Z. Hussein, R. Irmawati, S.B. Abd Hamid, *Catal. Today* (2004) 93-95, 715.

Y.H. Taufiq-Yap, M.H. Looi, K.C. Waugh, M.Z. Hussein, Z. Zainal, R. Samsuddin *Catal. Lett*. (2001) 74 (1-2) 99.

Y.H. Taufiq-Yap. and C.S Saw, *Effect of different calcinations environments on the vanadium phosphate for selective oxidation of propane and n-butane. Catal. Today.* (2007) 131, 285-291.

APPENDICES

Appendix A

Volume of 1-butanol Used

Molecular formula of vanadyl phosphate dihydrate = $VOPO_4{}_2H_2O$

Molecular weight of Vanadium = 50.9414 g/mol

Molecular weight of Phosphate = 30.97376 g/mol

Molecular weight of Oxygen = 15.9994 g/mol

Molecular weight of Hydrogen = 1.0079 g/mol

Molecular weight of $VOPO_4{}_2H_2O$ = 50.9414 g/mol + (7×15.9994 g/mol) + 30.97376 g/mol + (4×1.0079 g/mol)

= 197.94256 g/mol

No. of mol of $VOPO_4{}_2H_2O$ $= \frac{mass}{molecular\ weight}$

$= \frac{10\ g}{197.94256\ g/mol}$

= 0.05052 mol

(50 mol alcohol/ mol $VOPO_4{}_2H_2O$)

For 1 mol of $VOPO_4{}_2H_2O$, 50 mol of alcohol (1-butanol) is needed.

From the calculation as shown above, 0.05052 mol of $VOPO_4{}_2H_2O$ is used.

$$\frac{0.05052\ mol\ \mathrm{VOPO4 \cdot 2H2O}}{1\ mol\ \mathrm{VOPO4 \cdot 2H2O}} \times 50\ mol\ alcohol = 2.5260\ mol\ alcohol$$

Thus, 2.5260 mol of alcohol (1-butanol) is needed for 0.05052 mol of $VOPO_4{}_2H_2O$.

Molecular formula of 1-butanol = $C_4H_{10}O$

Molecular weight of Carbon = 12.011 g/mol

Molecular weight of Oxygen = 15.9994 g/mol

Molecular weight of Hydrogen = 1.0079 g/mol

Molecular weight of $C_4H_{10}O$ = (4×12.011 g/mol) + (10×1.0079 g/mol) + 15.9994 g/mol

= 74.1224 g/mol

Density of $C_4H_{10}O$ = 0.802 g/cm^3 at 20 ℃

Mass of $C_4H_{10}O$ = 74.1224 g/mol × 2.5260 mol

= 187.2332 g

Density $= \frac{mass}{volume}$

Volume of 1-butanol $= \frac{mass}{density}$

$= \frac{187.2332\ g}{0.802\ g/cm^3}$

= 233.4578 cm^3

Therefore, total volume of 1-butanol added is 233.4578 cm^3.

Appendix B

Volume of Distilled Water Used

(24 ml H_2O/ g solid)

15 g of V_2O_5 is used as a starting material.

Thus, the volume of distilled water needed = 15 g × (24 ml H_2O/ g solid)

= 360 ml

Appendix C

Crystallite Size Measurements by using Powder XRD Technique

Crystallite size, T given by Debye-Scherrer equation: T(Å) = $\frac{0.89\lambda}{FWHM \times cos\theta}$

Given $\lambda_{Cu\ K\alpha}$ = 1.54Å

FWHM (rad) = FWHM ( ) × $\frac{\pi}{180°}$

Appendix D

Preparation of Diphenylamine, Ph_2NH Indicator (Redox Titration)

1 g of diphenylamine was weighed and dissolved in a few ml of concentrated sulphuric acid, H_2SO_4. Then the solution was transferred to a 100 ml volumetric flask and further top up with concentrated H_2SO_4.

Appendix E

Preparation of 2 M Sulphuric Acid, H_2SO_4 Solution

Concentrated H_2SO_4 (95- 98%)

1L = 1.84 kg = 1840 g/ 1000cm^3 = 1.84 g/cm^3

Molecular weight of H_2SO_4 = 2(1.00 g/mol) + 32.07 g/mol + 4(16.00 g/mol)
= 98.07 g/mol

Concentration of 95- 98% H_2SO_4 = $\frac{1.84\ g/cm^3}{98.07\ g/mol} \times \frac{95}{100} \times 1000 = 17.82\ M$

$M_1V_1 = M_2V_2$ where M_1 = concentration of 95- 98% H_2SO_4
M_2 = concentration of diluted H_2SO_4 (2 M)
V_1 = volume of 95- 98% H_2SO_4
V_2 = volume of diluted H_2SO_4 (2 M)

(17.82 M) (V_1) = (2 M) (1000 cm^3)

V_1 = 112.23 cm^3

Appendix F

Preparation of 0.1 M Sulphuric Acid, H_2SO_4 Solution

$M_1V_1 = M_2V_2$ where M_1 = concentration of 95- 98% H_2SO_4

M_2 = concentration of diluted H_2SO_4 (0.1 M)

V_1 = volume of 95- 98% H_2SO_4

V_2 = volume of diluted H_2SO_4 (0.1 M)

$(17.82\ M)\ (V_1) = (0.1\ M)\ (1000\ cm^3)$

$V_1 = 5.61\ cm^3$

Appendix G

Preparation of 0.01 N Potassium Permanganate, $KMnO_4$ (Redox Titration)

Normality, N (eq/L) = M (mol/L) x *n* (eq/mol)

$MnO^{4-} + 8\ H^+ + 5\ e^- \leftrightarrow Mn^{2+} + 4\ H_2O$

$$\text{Molarity, M (mol/L)} = \frac{N(eq/L)}{n(eq/mol)}$$

$$= \frac{0.01}{5}$$

$= 0.002$ M

Molecular weight for $KMnO_4$ = 39.10 g/mol + 54.94 g/mol + 4 (16.00 g/mol)

= 158.04 g/mol

Weight for $KMnO_4$ in 1000 cm^3 diluted (0.1 M) H_2SO_4 = 0.002 x 158.04

= 0.3161 g

Appendix H

Preparation of 0.01 N ammonium iron(II) sulphate, $(NH_4)_2Fe(SO_4)_2 \cdot 6H_2O$ (Redox Titration)

Normality, N (eq/L) = M (mol/L) x *n* (eq/mol)

$Fe^{2+} + e^- \leftrightarrow Fe^{3+}$

Molarity, M (mol/L) $= \frac{N(eq/L)}{n(eq/mol)}$

$= \frac{0.01}{1}$

= 0.01 M

Molecular weight for $(NH_4)_2Fe(SO_4)_2 \cdot 6H_2O$ = 2 (14.00 g/mol) + 20 (1.00 g/mol) + 55.85 g/mol + 2 (32.07 g/mol) + 14 (16.00 g/mol)

= 391.99 g/mol

Weight for $(NH_4)_2Fe(SO_4)_2 \cdot 6H_2O$ in 1000 cm^3 diluted (0.1 M) H_2SO_4

= 0.01 x 392.14

= 3.9214 g

Appendix I

Oxidation State of Vanadium (Redox Titration)

Catalysts	V_{AV}	% of V^{4+}	% of V^{5+}
A	4.1241	87.59	12.41
B	4.2766	72.34	27.66
C	4.1111	88.89	11.11
D	4.1126	88.74	11.26

According to Niwa and Murakami (1982),

$T_1 = V^{4+} + 2V^{3+} = 20\,[MnO_4^-]\,V_1$ (1)

$T_2 = V^{5+} + V^{4+} + V^{3+} = 20\,[Fe^{2+}]\,V_2$ (2)

$T_3 = V^{5+} = 20\,[Fe^{2+}]\,V_3$ (3)

(2) – (3): $V^{3+} + V^{4+} = 20\,[Fe^{2+}]\,V_2 - 20\,[Fe^{2+}]\,V_3$ (4)

(1) – (4): $V^{3+} = 20\,[MnO_4^-]\,V_1 - 20\,[Fe^{2+}]\,V_2 + 20\,[Fe^{2+}]\,V_3$ (5)

Substitute (5) into (1):

$V^{4+} + 2(20\,[MnO_4^-]\,V_1 - 20\,[Fe^{2+}]\,V_2 + 20\,[Fe^{2+}]\,V_3) = 20\,[MnO_4^-]\,V_1$

$V^{4+} = 20\,[MnO_4^-]\,V_1 - 40\,[MnO_4^-]\,V_1 + 40\,[Fe^{2+}]\,V_2 - 40\,[Fe^{2+}]\,V_3$

$= 40\,[Fe^{2+}]\,V_2 - 40\,[Fe^{2+}]\,V_3 - 20\,[MnO_4^-]\,V_1$ (6)

Substitute (5) and (6) into (2):

$20\,[Fe^{2+}]\,V_2 = V^{5+} + (40\,[Fe^{2+}]\,V_2 - 40\,[Fe^{2+}]\,V_3 - 20\,[MnO_4^-]\,V_1) + (20\,[MnO_4^-]\,V_1 - 20\,[Fe^{2+}]\,V_2 + 20\,[Fe^{2+}]\,V_3)$

$V^{5+} = 20\,[Fe^{2+}]\,V_3$ (7)

From (5): V^{3+} $= 20\ (0.01)\ V_1 - 20\ (0.01)\ V_2 + 20\ (0.01)\ V_3$

$= 0.2\ (V_1 - V_2 + V_3)$ (8)

From (6): V^{4+} $= 40\ (0.01)\ V_2 - 40\ (0.01)\ V_3 - 20\ (0.01)\ V_1$

$= 0.4\ V_2 - 0.4\ V_3 - 0.2\ V_1$ (9)

From (7): V^{5+} $= 20\ (0.01)\ V_3$

$= 0.2\ V_3$ (10)

The average vanadium valence is calculated as:

$$V_{AV} = \frac{3V^{3+} + 4V^{4+} + 5V^{5+}}{V^{3+} + V^{4+} + V^{5+}} \quad (11)$$

Sample A

$V_1 = 10.15$, $V_2 = 11.10$, $V_3 = 1.33$

From (6): V^{4+} $= 40\ (0.01)\ V_2 - 40\ (0.01)\ V_3 - 20\ (0.01)\ V_1$

$= 0.4\ V_2 - 0.4\ V_3 - 0.2\ V_1$

$= 0.4\ (11.10) - 0.4\ (1.33) - 0.2\ (10.15)$

$= 1.878$

From (7): V^{5+} $= 20\ (0.01)\ V_3$

$= 0.2\ V_3$

$= 0.2\ (1.33)$

$= 0.266$

The average vanadium valence is calculated as:

$$V_{AV} = \frac{3V^{3+} + 4V^{4+} + 5V^{5+}}{V^{3+} + V^{4+} + V^{5+}}$$

$$= \frac{3(0) + 4(1.878) + 5(0.266)}{0 + 1.878 + 0.266}$$

$$= 4.1241$$

If V_{AV} of sample A= 4.1241

V^{5+} (%) = 12.41 %

V^{4+} (%) = (100 – 12.41) %

= 87.59 %

Sample B

V_1 = 8.60, V_2 = 11.30, V_3 = 3.033

From (6): V^{4+} = 40 (0.01) V_2 - 40 (0.01) V_3 - 20 (0.01) V_1

= 0.4 V_2 – 0.4 V_3 – 0.2 V_1

= 0.4 (11.30) – 0.4 (3.033) – 0.2 (8.60)

= 1.5868

From (7): V^{5+} = 20 (0.01) V_3

= 0.2 V_3

= 0.2 (3.033)

= 0.6066

The average vanadium valence is calculated as:

$$V_{AV} = \frac{3V^{3+} + 4V^{4+} + 5V^{5+}}{V^{3+} + V^{4+} + V^{5+}}$$

$$= \frac{3(0) + 4(1.5868) + 5(0.6066)}{0 + 1.5868 + 0.6066}$$

$$= 4.2766$$

If V_{AV} of sample B = 4.2766

V^{5+} (%) = 27.66 %

V^{4+} (%) = (100 – 27.66) %

= 72.34 %

Sample C

V_1 = 11.30, V_2 = 12.15, V_3 = 1.30

From (6): V^{4+} = 40 (0.01) V_2 - 40 (0.01) V_3 - 20 (0.01) V_1

= 0.4 V_2 – 0.4 V_3 – 0.2 V_1

= 0.4 (12.15) – 0.4 (1.30) – 0.2 (11.30)

= 2.08

From (7): V^{5+} = 20 (0.01) V_3

= 0.2 V_3

= 0.2 (1.30)

= 0.26

The average vanadium valence is calculated as:

$$V_{AV} = \frac{3V^{3+} + 4V^{4+} + 5V^{5+}}{V^{3+} + V^{4+} + V^{5+}}$$

$$= \frac{3(0) + 4(2.08) + 5(0.26)}{0 + 2.08 + 0.26}$$

$$= 4.1111$$

If V_{AV} of sample C = 4.1111

V^{5+} (%) = 11.11 %

V^{4+} (%) = (100 – 11.11) %

= 88.89 %

Sample D

V_1 = 10.85, V_2 = 11.85, V_3 = 1.30

From (6): V^{4+} = 40 (0.01) V_2 - 40 (0.01) V_3 - 20 (0.01) V_1

= 0.4 V_2 – 0.4 V_3 – 0.2 V_1

= 0.4 (11.85) – 0.4 (1.30) – 0.2 (10.85)

= 2.05

From (7): V^{5+} = 20 (0.01) V_3

= 0.2 V_3

= 0.2 (1.30)

= 0.26

The average vanadium valence is calculated as:

$$V_{AV} = \frac{3V^{3+} + 4V^{4+} + 5V^{5+}}{V^{3+} + V^{4+} + V^{5+}}$$

$$= \frac{3(0) + 4(2.05) + 5(0.26)}{0 + 2.05 + 0.26}$$

$$= 4.1126$$

If V_{AV} of sample C = 4.1126

V^{5+} (%) = 11.26 %

V^{4+} (%) = (100 – 11.26) %

= 88.74 %

Appendix J: Computer Generated Data